



HAL
open science

H₂S chemical looping selective and preferential oxidation to sulfur by bulk V₂O₅

Tanushree Kane, Jesùs Guerrero-Caballero, Axel Löfberg

► **To cite this version:**

Tanushree Kane, Jesùs Guerrero-Caballero, Axel Löfberg. H₂S chemical looping selective and preferential oxidation to sulfur by bulk V₂O₅. *Applied Catalysis B: Environmental*, 2020, 265, pp.118566. 10.1016/j.apcatb.2019.118566 . hal-02926555

HAL Id: hal-02926555

<https://hal.univ-lille.fr/hal-02926555>

Submitted on 31 Aug 2020

HAL is a multi-disciplinary open access archive for the deposit and dissemination of scientific research documents, whether they are published or not. The documents may come from teaching and research institutions in France or abroad, or from public or private research centers.

L'archive ouverte pluridisciplinaire **HAL**, est destinée au dépôt et à la diffusion de documents scientifiques de niveau recherche, publiés ou non, émanant des établissements d'enseignement et de recherche français ou étrangers, des laboratoires publics ou privés.

H₂S chemical looping selective and preferential oxidation to sulfur by bulk

V₂O₅

Tanushree Kane, Jesús Guerrero-Caballero, Axel Löfberg

Univ. Lille, CNRS, Centrale Lille, ENSCL, Univ. Artois, UMR 8181 - UCCS - Unité de Catalyse et

Chimie du Solide, F-59000 Lille, France

Keywords- V₂O₅, H₂S selective oxidation, chemical looping, oxygen carrier

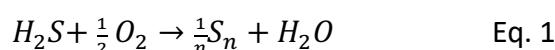
Abstract

The concept of chemical looping is applied for the first time to selective oxidation of H₂S to elemental sulfur. An oxygen carrier (OC) is exposed to cyclic reduction by H₂S and oxidation by O₂. The properties of bulk V₂O₅ as OC are explored for this reaction in the 150-200 °C temperature range. Steady cyclic behavior can be obtained with high selectivity towards elemental sulfur. Some undesired SO₂ is formed during exposure to H₂S but more significantly during re-oxidation of the OC. This indicates that bulk V₂O₅ does not completely oxidize the adsorbed H₂S in the reductant step. Characterizations indicate that V⁴⁺ and V⁵⁺ species are mostly involved in the process. Preferential oxidation in presence of CH₄ is confirmed on this OC. Although optimization needs to be done, the potential of chemical looping concept for direct preferential oxidation of H₂S in natural gas and biogas is demonstrated.

1.Introduction

Removal of sulfur-containing compounds is one of the main issues in the fuel industry. H₂S is one of the significant compounds to be considered as gasoline or diesel desulfurization processes generate a large amount of this gas. Natural gas and biogas also contain large amounts of H₂S (tens to hundreds of ppm), which must be removed before the fuels can be used as energy sources or chemical feedstock.

The Claus process is a well-known process for converting H₂S to elemental sulfur at a large industrial scale [1]. However, the recovery of sulfur in the Claus process is not complete due to the overall limitation of thermodynamic equilibrium leading to only 95-97 % of sulfur recovery. To remove the residual H₂S, various processes of additional purification are needed. Therefore, this process is uneconomical for small plants and not suitable for gas streams with low concentrations of H₂S. Furthermore, in the case of natural or biogas treatment, H₂S needs to be separated from the mainstream before being processed. The most attractive method to treat the H₂S is the selective catalytic oxidation of H₂S to elemental sulfur (Eq. 1).



As H₂S selective oxidation to elemental sulfur is an exothermic reaction, this reaction is irreversible and does not have any equilibrium limitations contrary to the Claus process. Yield towards elemental sulfur is usually limited by SO₂ which can be formed as a major by-product depending on the ratio of H₂S to O₂, reaction temperature and catalyst efficiency. Side reactions, such as elemental sulfur deposition or deactivation of the active phase, are generally responsible for the alteration of sulfur yield with time. To avoid sulfur deposition inside the catalytic reactor, reaction needs to be performed above 150-180 °C. Different

vanadium-based catalysts have already been studied in the past [2-5]. In particular, bulk V_2O_5 phase has been reported to have a better performance than other bulk oxides like magnesium oxide, bismuth oxide, and molybdenum oxide, iron oxide [6-8].

Vanadium oxide catalysts have been extensively studied for many hydrocarbon oxidation reactions, mostly as supported catalysts, for example by Wachs et al. [9, 10]. Characterization studies have revealed that the deposited vanadium phase contains two-dimensional surface vanadium along with V_2O_5 crystallites above monolayer coverage. Vanadium catalysts also show important redox properties and ability to react at low temperature. The reactivity properties of the supported vanadium catalysts were compared with the structural properties of the dehydrated surface V^{5+} species rather than the dehydrated reduced surface vanadia V^{4+} and V^{3+} species. Apart from this, the importance of the role of the terminal $V=O$ bond as well as that of bridging $V-O-V$ bond was shown in the case of selective oxidation of hydrocarbons. The surface concentration of bridging $V-O-V$ bonds increases with vanadia coverage due to the increase in the ratio of polymerized to isolated vanadia species. Doping of the vanadium catalysts by various metals like Mo, La, Cu, Ce has been studied in detail [8,11-14] and showed the effect of these metals on the vanadium species and hence on the activity and selectivity of the catalysts.

Chemical looping (CL) processes attract increasing interest with time to understand and implement this concept in different oxidation reactions. CL processes involve an oxygen carrier, which is reduced in the presence of a reductant and produces the desired product. Subsequently, the exposure of the reduced solid to an oxidant allows the carrier re-oxidation and regeneration. Although many of the elementary steps involved in CL operations are similar to catalytic reactions (reactant adsorption, surface reactivity, product desorption), it

should be emphasized that the oxygen carrier material acts as an actual reactant and not as a catalyst [15]. For CL, original reactor systems are necessary with respect to classical co-feed fixed (or fluidized) bed reactors. For solid oxygen carriers and gas phase reactants, CL generally involves the use of circulating fluidized bed systems [16] or fixed bed switching reactors. For the experimental studies in the laboratory scale, the fixed bed reactor which is fed alternatively with the gas reactants is usually the most appropriate while circulating bed reactor systems are better adapted for industrial applications as already used in Fluid Catalytic Cracking (FCC) for example [17,18].

Although CL processes have been studied for several reactions of industrial interest by Löfberg et al. [19], Bhavsar et al. [20], Ma et al. [21] or Pachler et al. [22], for example. To our knowledge, the concept of CL oxidation of H₂S to elemental sulfur has never been proposed.

It consists of separating Eq. 1 in two distinct steps:



Where “OC” represents the oxygen carrier.

Such an approach could offer important advantages with respect to direct, co-feed, oxidation reaction:

- provided an appropriate OC carrier is developed, selectivity could be improved by avoiding direct interaction between adsorbed sulfur species and di-oxygen from the gas phase or adsorbed on the surface of the material and favoring the reactivity of lattice oxygen species;

- eventual sulfur species deposited on the surface of the carrier could be removed during regeneration step thus limiting the deactivation of the process;
- no mixing of H_2S and O_2 can improve the safety of the process and enlarge considerably the range of H_2S concentrations which may be considered, including even pure H_2S ;
- depending on the reactivity of the oxygen carrier material and reaction conditions, oxidation of H_2S could be performed in the presence of other combustible gases such as methane.

In this last case, if preferential oxidation of H_2S is achieved in the presence of methane, then the direct purification of natural or bio-gas could be performed without the need for prior separation of H_2S . This would constitute a significant breakthrough in natural and bio-gas treatment.

The key to such development is in the oxygen carrier, which needs to fulfill specific requirements. It should have:

- high reactivity in both the H_2S oxidation and the regeneration steps;
- good selectivity for the desired oxidation product, i.e. elemental sulfur;
- good stability over many of redox cycles;
- good resistance towards sulfur deposition and removal.

For industrial implementation of the process, other properties will obviously be required, such as good mechanical resistance in circulating bed systems.

As reminded, V_2O_5 is well known for its redox properties and catalytic reactivity for H_2S oxidation [2,23-24]. For this reason, bulk V_2O_5 was chosen as OC to explore this new approach towards H_2S oxidation by chemical looping.

In a first step, the thermodynamics of the system are considered to check the feasibility of operating in CL mode for this reaction using V_2O_5 . Then the reactivity of the carrier is studied versus temperature and exploring different H_2S concentrations and $H_2S:O_2$ ratio. Finally, the chemical looping is performed in presence of methane to check if preferential oxidation of H_2S can be achieved.

2. Experimental section

2.1 Carrier synthesis

Vanadium oxide was prepared in the laboratory by calcining the precursor (ammonium metavanadate - Sigma Aldrich). Stepwise heating of the precursor was done in the presence of N_2 until 200 °C, then it heated until 500 °C at 5 °C min^{-1} in the presence of O_2 . The dark orange color powder obtained at the end of the calcination shows the presence of V_2O_5 .

2.2 Carrier characterization

The XRD patterns of the different materials were obtained using a D8 Advanced Bruker AXS diffractometer. The wavelength of $CuK\alpha_1$ X-ray radiation used was 1.5418 Å. The configuration for Bragg-Brentano diffractometer was theta-2 theta. The samples were immobilized on ceramic glass (Macor) holders. The angle (2θ) of XRD was varied between 10 and 80° with a step size of 0.02° and an integration time of 3 s.

N₂ physisorption at 77 K data was collected on multipoint and single point equipment to obtain the surface area of the different catalysts before the test.

XPS analysis was performed using a Kratos Analytical AXIS UltraDLD spectrometer. A monochromatized aluminum source (AlK α =1486.6 eV) was used for excitation. The X-ray beam diameter is around 1 mm. The analyzer was operated in constant pass energy of 40 eV using an analysis area of approximately 700×300 μ m. Charge compensation was applied to compensate for the charging effect occurring during the analysis. The C 1s (2848 eV) binding energy (BE) was used as an internal reference. The spectrometer BE scale was initially calibrated against the Ag 3d_{5/2} (368.2 eV) level. Pressure was in the 10⁻¹⁰ Torr range during the experiments. Simulation of the experimental photopeaks was carried out using Casa XPS software. Quantification considered a nonlinear Shirley background subtraction.

Raman spectra were recorded at room temperature with the 647.1 nm excitation line from a Spectra Physics krypton ion laser with 3 mW laser power at the sample. The beam was focused on the compounds using the macroscopic configuration. The scattered light was analyzed with an XY 800 Raman Dilor spectrometer equipped with an optical multichannel detector (liquid nitrogen-cooled charge coupled device). The spectral resolution was approximately 0.5 cm⁻¹ in the investigated 200-1000 cm⁻¹ range.

2.3 Reactivity tests for H₂S selective oxidation.

A detailed description of the reactor setup, together with a scheme (Fig. S1), is provided in Supplementary Information. In summary, premixed gas cylinders containing 1 mol% H₂S in He and 10 mol% O₂ in He were used and mixed to pure Ar. As Helium is fed together with reactants with known ratio, it serves as a diluent but also as a tracer for conversion

calculations. For a H₂S:O₂ ratio of 1:5, H₂S/He (5 mL min⁻¹) was passed through the reactor together with 95 mL min⁻¹ of Ar during so-called “reductant step” and O₂/He (10 mL min⁻¹) together with 90 mL min⁻¹ of Ar during so-called “oxidant step”. Between these steps, 100 mL.min⁻¹ Ar was passed through the reactor in order to maintain the reactor under a constant total flow ($F_T = 100 \text{ ml min}^{-1}$). For other H₂S:O₂ ratio, the gas flow rates were adapted consequently. All flow rates were set using mass flow controllers (5980 Brooks) and reactions were performed at atmospheric pressure.

A glass tube maintained at room temperature was placed at the outlet of the reactor in order to condensate the elemental sulfur produced and to avoid plugging of the mass spectrometer inlet.

<p><i>Table 1. Operating condition for Chemical looping process</i></p>

The general operating conditions are summarized in Table 1. The concentration of the H₂S was varied from the 1000 ppm (100 Pa) to 4000 ppm (400 Pa). For most of the study H₂S:O₂ was maintained at 1:5, i.e. O₂ is varied from 5000 ppm (500 Pa) to 20000 ppm (2000 Pa) according to H₂S concentration. H₂S:O₂ ratios of 1:2.5 and 1:0.5 were explored as well.

The temperature range explored is between 150 and 250 °C. Typically, 80 mg of V₂O₅ was used and diluted in inert material (SiC). Between experiments, regeneration treatments of the carrier are performed by exposing the solid to diluted O₂ (1%) and heating the sample to 400 °C for 30 minutes to fully re-oxidize the carrier and eventually remove adsorbed sulfur species.

Preferential oxidation of H₂S in presence of methane was tested. 20 mL min⁻¹ was added in the reductant step and the Ar flow adjusted to maintain the total flow rate at 100 mL min⁻¹. Reactivity of V₂O₅ with respect to methane alone was also tested by exposing the OC to 20% of methane and 5% of O₂ in a cyclic manner in the absence of H₂S in the 150-500°C temperature range.

In chemical looping operation, the reactivity of systems is directly linked to gas phase reactant feed (thus to concentration and flow rate), amount of carrier and duration of exposure of carrier to each reactant. Considering carrier bed volume (1 mL) and typical gas flow rate ($F_T = 100 \text{ mL min}^{-1}$) the gas contact time (i.e. time during which single H₂S or O₂ molecules are exposed to solid) can be estimated to 0.6 s. On the other hand, the time during which the solid is exposed to the reactant gas is dependent on cyclic programming. In this study, each cycle consisted of exposing the sample to reductant (H₂S) and oxidant (O₂) for 1 min each with an interval of 2 min in Ar.

Cycles were repeated 20 or 30 times. During the first and the last cycle of the reaction, the reactor was closed to get the reference bypass value for background definition and sensitivity determination for Ar, He, H₂S and O₂ of the online quadrupole mass analyzer (Omnistar 200, Pfeiffer Vacuum). SO₂ sensitivity was determined and checked regularly using a calibrated gas mixture.

Figure S2a illustrates a typical example gas phase composition evolution with time during CL operation in these experimental conditions. Figure S2b shows a detail of last cycle in presence of carrier and by-pass (reference) cycle.

Quantitative information can be obtained in different parts of the cycles. In the reductant step, H₂S conversion **X_{H₂S} (%)** is obtained by integrating the outlet H₂S flow and comparing this to the theoretical H₂S inlet calculated using the He tracer.

$$X_{H_2S}(\%) = \frac{(H_2S(inlet(\mu mol)) - H_2S(outlet(\mu mol)))}{H_2S(inlet(\mu mol))} \times 100 \quad \text{Eq. 4}$$

In the oxidant step, O₂ conversion **X_{O₂} (%)** is obtained by integrating the outlet O₂ flow and comparing this to the theoretical O₂ inlet calculated from the He tracer.

$$X_{O_2}(\%) = \frac{(O_2(inlet(\mu mol)) - O_2(outlet(\mu mol)))}{O_2(inlet(\mu mol))} \times 100 \quad \text{Eq. 5}$$

SO₂ can be produced in both reductant and oxidant steps. **S_{SO₂R} (%)** represents SO₂ selectivity **in the reductant step** (amount of SO₂ formed in the presence of H₂S and following inert gas divided by amount of converted H₂S) and is indicative of direct unselective oxidation of H₂S by the oxygen carrier.

$$S_{SO_2R}(\%) = \frac{SO_{2(R)}(\mu mol)}{(H_2S(inlet(\mu mol)) - H_2S(outlet(\mu mol)))} \times 100 \quad \text{Eq. 6}$$

S_{SO₂O} (%) represents SO₂ selectivity in oxidant phase (amount of SO₂ formed in presence of O₂ and following inert gas divided by amount of converted H₂S and represents the oxidation of sulfur species which remain adsorbed at the surface of the carrier after the reductant step.

$$S_{SO_2O}(\%) = \frac{SO_{2(O)}(\mu mol)}{(H_2S(inlet(\mu mol)) - H_2S(outlet(\mu mol)))} \times 100 \quad \text{Eq. 7}$$

As S formation cannot be monitored directly from the mass spectrometer, the selectivity towards S can only be calculated indirectly considering the total SO₂ formed on the overall

cycle and considering that no S accumulates on the carrier along cycling. Thus, $S_{SO_2} T$ (%) represents the total SO₂ selectivity:

$$S_{SO_2} T = S_{SO_2} R + S_{SO_2} O \quad \text{Eq. 8}$$

And selectivity to S is obtained as follows:

$$S = 100 - S_{SO_2} T \quad \text{Eq. 9}$$

Considering the amount of S and SO₂ produced during the reductant step, and taking into account the theoretical amount of corresponding H₂O, it is possible to calculate the overall amount of O atoms involved for a single reductant step. On the other hand, the overall amount of lattice oxygen present in the OC can be calculated knowing the solid composition (i.e. V₂O₅). By making the hypothesis that only 1 out of 5 oxygen atoms is involved (corresponding to the reduction of V⁵⁺ to V⁴⁺) one can calculate the amount of lattice oxygen (%O_{latt}) involved in the reductant step.

All data are obtained with a relative error margin of 5 %.

3. Results

3.1 Thermodynamic of V₂O₅ reduction by H₂S and re-oxidation by O₂

For V₂O₅, the variation of Gibbs free energy of oxide reduction by H₂S calculated for the numerous partially reduced phases reported in the V-O phase diagram. However, the number of partially reduced phases for which thermodynamic data is available is limited, even if the redox properties of V₂O₅ have been already studied extensively in catalysis. Using standard Gibbs free energy ($\Delta_r G^\circ$) data using FactSage database [25], $\Delta_r G^\circ$ have been calculated for V₂O₅ (V⁵⁺) reduction by H₂S to VO₂ (V⁴⁺) and V₂O₃ (V³⁺) oxides considering selective (green

symbols) or total oxidation (black symbols) and represented in Figure 1 at different temperatures.

Figure 1: Variation of standard Gibbs free energy with temperature for H₂S oxidation by V₂O₅.

Reduction of V₂O₅ by H₂S to VO₂ (closed symbols) or V₂O₃ (open symbols), selective oxidation to S (green), unselective to SO₂ (black), carrier re-oxidation by O₂ (red), co-feed reaction in brown with

H₂S:O₂ = 1:5 and 1:0.5 (brown), VOSO₄ formation (blue)

Re-oxidation of the reduced oxides has also been considered (red symbols). Within the temperature range of interest for our experiments (150 – 250 °C), the reduction of the V₂O₅ to VO₂ and V₂O₃ by H₂S producing selectively elemental S is always thermodynamically possible and not very sensitive to temperature. The re-oxidation of the corresponding reduced phases is also feasible. The $\Delta_f G^\circ$ for total oxidation is always significantly more exothermic than selective oxidation, meaning that the reaction kinetics will play the vital role on the overall reactivity of the system. One should also mention that the formation of vanadyl sulfate (VOSO₄) is also thermodynamically feasible in the reaction conditions. Values for co-feed catalytic oxidation are also reported for comparison.

From this data, it can be concluded that in all reaction conditions explored in this work, total conversion of H₂S to SO₂ will always be the most favorable reaction, both in chemical looping and co-feed modes. Furthermore, attention will need to be made on the possible formation of VOSO₄.

3.2. Performances in co-feed catalytic H₂S selective oxidation.

Co-feed catalytic oxidation of H₂S by bulk V₂O₅ has been performed at 150 °C and 200 °C using different H₂S:O₂ ratio. Ratio 1:0.5 corresponds to the stoichiometric ratio for selective oxidation to elemental sulfur (Eq. 1). At such low ratio, unselective oxidation to SO₂ is less favored and best selectivity to H₂S is expected. On the other hand, chemical looping experiments were performed at higher O₂ concentration (H₂S:O₂ = 1:5). For this reason, co-feed experiments have been performed at both ratio 1:5 and 1:0.5. All co-feed performances are summarized in Table 2 while conversion/selectivity evolution with time are illustrated in Figures S3A and S3B.

<i>Table 2. Co-feed catalytic oxidation of H₂S on bulk V₂O₅; 80 mg V₂O₅ + 900 mg SiC, F_T = 100 mL min⁻¹.</i>

As it could be expected, bulk V₂O₅ is active for H₂S oxidation and total conversion of H₂S can be observed initially in all conditions. Generally, experiments made with stoichiometric ratio show better selectivity to S compared to those performed in excess O₂ in line with what is generally observed for this reaction.

In particular for excess oxygen conditions, temperature has a considerable effect on SO₂ selectivity. Low temperature experiments show better performances in term of selective oxidation but suffer from rapid deactivation. In excess oxygen (H₂S:O₂ = 1:5), 10% of conversion is lost in 30 minutes reaction time while SO₂ selectivity increases significantly. Conversion then continues to decrease but selectivity remains stable. At lower oxygen feed, the deactivation process is more rapid 20% conversion loss in 30 minutes, 42% loss in 72%

minutes) but selectivity remains stable. Figures S2B indicates that the deactivation process in these conditions is complex and can involve both poisoning by S containing species and evolution of the solid (reduction, VO_2 formation, ...).

3.3. Performances in Chemical looping H_2S selective oxidation.

Bulk V_2O_5 has been tested in chemical looping selective oxidation of H_2S and over 20 cycles. Although at 150 and 200 °C sulfur should be in liquid state, several factors should be taken in consideration: (i) S vapor pressure is low but not negligible in the temperatures considered (approx. 200 to 2000 ppm at 150 and 200 °C, respectively), (ii) feed in H_2S (and thus S formation) in intermittent on the contrary to co-feed reaction and (iii) the actual gas temperature is probably higher than 150 or 200 °C due to the heat of reactions. These factors contribute to the vaporization of S and its condensation at the outlet of reactor in an unheated zone (glass condenser) as this could be visually observed in all cases.

H_2S conversion and selectivity to S and SO_2 are represented in Figure 2. Each point represents the reactivity integrated over a full cycle.

All quantitative results in different reaction conditions are summarized in Table 3. Here, net amounts of reacted H_2S and produced SO_2 are also indicated together with conversions and selectivity. H_2S conversion remains above 80% during the experiment with a decrease of 8% with cycling. SO_2 is produced during both reductant and oxidant steps. In both cases, SO_2 production slightly decreases during the initial 5 cycles; afterward it reaches a stable value. Correspondingly the selectivity towards sulfur formation increases from 72% to 85%.

*Figure 2. Chemical looping oxidation of H₂S; 80 mg V₂O₅ + 900 mg SiC at 150 °C, F_T = 100 mL min,
Cycle: 1 min. in 2000 ppm of H₂S, and 1 min. in O₂ of 10000 ppm of O₂ (H₂S:O₂ = 1:5)*

These results confirm that V₂O₅ is a potential active phase for selective oxidation of H₂S in chemical looping mode, although performances clearly need to be optimized. In particular, stable and repetitive reactivity need to be obtained by better understanding the nature of the deactivation process. Furthermore, the overall selectivity to S needs to be improved by:

- (i) lowering SO₂ formation in the reductant step and,
- (ii) limiting the amount of unreacted adsorbed species which are oxidized in oxidant step forming SO₂.

3.3.1 Effect of the Temperature

The evolution of the H₂S conversion during the reductant step at 150 and 200 °C can be seen in Figure 3A. The evolution of selectivity is reported in Figure 3B while the overall performances during the last cycles are represented in Figure 4.

*Figure 3. Chemical looping oxidation of H₂S; 80 mg V₂O₅ + 900 mg SiC at 150 °C, F_T = 100 mL min,
Cycling: 1 min. in 2000 ppm of H₂S, and 1 min. in O₂ of 10000 ppm of O₂ (H₂S:O₂ = 1:5)
A: H₂S conversion, B: SO₂ selectivity (in reductant steps, oxidant steps and overall)*

Figure 4. Chemical looping oxidation of H₂S, overall performance at 20 cycles; 80 mg V₂O₅ + 900 mg SiC at 150 °C, F_T = 100 mL min⁻¹; Cycling: 1 min. in 2000 ppm of H₂S, and 1 min. in O₂ of 10000 ppm of O₂ (H₂S:O₂ = 1:5)

Initial H₂S conversion is slightly higher at 200 °C than at 150 °C, but at both temperatures, it decreases with the cycles and reaches similar values near 80%. It should be noted that this is an integrated conversion on the full exposure time to H₂S. As seen in Figures 5A and 5B, during the reductant steps an evolution of the unreacted H₂S is observed, specifically at 200 °C. This means that if the steps had been shorter, the integrated conversion would have given higher overall values. Regarding SO₂ production, as already seen previously, the overall SO₂ production at 150 °C decreases slightly during the first cycles then reaches stable values.

Figure 5. Detailed gas evolution during cycling; 80 mg V₂O₅ + 900 mg SiC at 150 °C, F_T = 100 mL min⁻¹; Cycling: 1 min. in 2000 ppm of H₂S, and 1 min. in O₂ of 10000 ppm of O₂ (H₂S:O₂ = 1:5)
A: 150°C and B: 200°C

At high temperature (200 °C) initial selectivity to SO₂ in the reductant step is very high (approx. 25 %) with respect to 150 °C (7-8%) and decreases steadily with cycling to reach approx. 17-18 % after 20 cycles. On the contrary, SO₂ formed in the oxidant step starts at a very low value and increases continuously with cycling. This indicates that an increasing proportion of H₂S adsorbed during reductant step is not converted to either SO₂ or S in this step but oxidized to SO₂ in oxidant step. This could indicate that the regeneration of the

oxygen capacity of the carrier is not complete to ensure a stable and reproducible reactivity along with cycling. Interestingly, such evolution is observed at higher temperature while it could be expected that the regeneration should be facilitated by the increase of temperature. Obviously, SO_2 produced in oxidant step necessarily comes from the oxidation of sulfur containing species which remained adsorbed after reductant step. The nature of these species is however not known in absolute. However, it is interesting to note that water is produced during the oxidant step meaning that the sulfur containing species which remain adsorbed between the reductant and oxidant step are not fully dehydrogenated. It is therefore more likely that H_2S remain adsorbed than elemental S.

Table 3. Summary of the results for CL oxidation of H_2S in various experimental conditions; 80 mg V_2O_5 + 900 mg SiC; $T = 150$ or 200 °C; H_2S concentration = 1000, 2000 or 4000 ppm; $\text{H}_2\text{S}:\text{O}_2$ ratio = 1:5, 1:2.5 or 1:0.5

3.3.2 Effect of the H_2S concentration at 150 °C

Figure 6 shows the evolution of the activity and selectivity at 150°C at 1000, 2000, 4000 ppm of H_2S concentration along with cycling.

Figure 6. Chemical looping oxidation of H₂S with different H₂S-O₂ concentrations; 80 mg V₂O₅ + 900 mg SiC at 150°C, F_T = 100 mL min⁻¹; Cycling: 1 min. in H₂S (4000, 2000, 1000 ppm) and 1 min. in O₂

(H₂S:O = 1:5)

A: H₂S conversion, B: SO₂ selectivity in reductant step, C: SO₂ selectivity in oxidant step, D: overall SO₂ selectivity

At low concentration (1000 ppm), a high conversion of H₂S is observed with high selectivity towards the sulfur formation. A slight decrease of conversion with cycling is observed but the formation of the SO₂ in the reductant and oxygen step is practically constant throughout the experiment, which illustrates the good regeneration of the catalysts during the reaction.

In terms of H₂S conversion and selectivity toward SO₂ in the reductant step, the behavior observed at 1000 ppm of H₂S is very similar to that observed at 2000 ppm already seen in previous sections. The only difference is a slightly lower selectivity to SO₂ in the oxidant step at lower H₂S concentration indicating that less adsorbed species remains at the end of the reductant step when lower concentrations of H₂S are used. On the contrary, when increasing the H₂S concentration to 4000 ppm, initial conversion is high (80 %) but decreases significantly to reach a stable value around 60%. The selectivity towards SO₂ in the reductant step is low and remarkably similar to that observed with lower H₂S concentrations. However, the amount of SO₂ produced in oxidant step increases strongly, indicating that the full conversion of all adsorbed species is limited in the reductant step leading to more residual sulfur containing species oxidized in the oxidant step.

Figure 7 summarizes the performances reached during the last cycles and illustrates the decrease of conversion observed at increasing H₂S inlet concentration. Selectivity in reductant step does not seem affected by inlet concentration, on the contrary to SO₂ formation in oxidant step which increases with H₂S concentration. This suggests that species adsorbed during reductant step either react to form selectively elemental sulfur and small amounts of SO₂, or remain adsorbed and are converted to SO₂ in oxidant step. The increase in H₂S concentration, in particular from 2000 to 4000 suggest that the maximum amount of H₂S that can actually be converted in reductant step is reached in these conditions of carrier amount and temperature.

Figure 7. Overall performances during last cycles; 80 mg V₂O₅ + 900 mg SiC at 150°C, F_T = 100 mL min⁻¹

1.

Cycle: 1 min. in H₂S (4000, 2000, 1000 ppm) and 1 min. in O₂, H₂S:O₂- 1:5

3.3.3 Effect of different reactant ratio

The effect of different ratio of reactants has been studied at 150 °C by keeping the H₂S concentration at 2000 ppm and changing the oxygen concentration from 10000 ppm to 5000 ppm and 1000 ppm to achieve H₂S:O₂ ratio of 1:5, 1:2.5 and 1:0.5 respectively. The 1:0.5 ratio corresponds to the stoichiometric one for selective oxidation of H₂S (Eq. 1). The evolution of the activity and selectivity along cycling are presented in Figures 8.

For each ratio, H₂S conversion varies with time (Figure 8A). In the case of ratio 1:2.5, the slope of conversion evolution with cycles is steeper than using 1:5 ratio. The initial slope of

deactivation is even steeper using the stoichiometric ratio of 1:0.5, but in this case, activity reaches a stable value after approx. 10 cycles.

Except during the very first cycles of each experiment, the selectivity towards SO₂ in the reductant step is very stable and unaffected by the O₂ concentration (Figure 8B).

Figure 8. Chemical looping oxidation of H₂S with different H₂S:O₂ ratio, 80 mg V₂O₅ + 900 mg SiC at 150°C, F_T = 100 mL min⁻¹, Cycling: 1min. in 2000 ppm of H₂S, and 1 min. in O₂; H₂S:O₂ = 1:5, 1:2.5,

1:0.5

A: H₂S conversion, B: SO₂ selectivity in reductant step, C: SO₂ selectivity in oxidant step, D: overall

SO₂ selectivity

Different trends are observed for SO₂ formation during the oxidant step (Figure 8C). It significantly decreases at highest O₂ concentration (H₂S:O₂ = 1:5) while it increases for intermediate H₂S:O₂ ratio (1:2.5). Both these cases correspond to experiments performed in large excess of oxygen with respect to ideal reaction (Eq. 1) and, interestingly, selectivity to SO₂ formation in oxidant step reach similar values (12-13 %). At the lowest O₂ concentration (H₂S:O₂ = 1:0.5), this selectivity it is remarkably stable around 5%. In this case, the H₂S:O₂ ratio (1:0.5) corresponds to the stoichiometric one for selective oxidation (Eq 1) and O₂ conversion is actually very high (Figure 9) and could explain the low selectivity to SO₂ in oxidant step.

It can be noted that although the O₂ concentration decreases by a factor 10 between the ratio 1:5 to the ratio 1:0.5, the overall amount of lattice oxygen involved (%O_{latt}, Table 3) in the process decreases only very slightly in line with the decrease of overall conversion.

Figure 9 summarizes the performances reached during the last cycles. It indicates clearly that the selectivity towards SO₂ in reductant step is not influenced by oxygen concentration in oxidant step. However, total conversion of H₂S decreases with decreasing O₂ concentration suggesting that the efficiency of the regeneration is not complete in these conditions.

Figure 9. Overall performances during last cycle with different H₂S:O₂ ratio; 80 mg V₂O₅ + 900 mg SiC at 150°C, F_T = 100 mL min⁻¹, Cycle: 1min. in 2000 ppm of H₂S, and 1 min. in O₂; H₂S:O₂ = 1:5 (20th cycle), 1:2.5 (30th cycle), 1:0.5 (30th cycle)

3.3.4 Reactivity in presence of methane

The chemical looping experiments were also performed by feeding methane simultaneously with H₂S during reductant step to verify if preferential oxidation of H₂S could be achieved. Results obtained in similar experimental conditions with and without CH₄ in reductant feed are presented in Figure S4. No traces of products indicative of CH₄ reactivity (CO, CO₂, CS₂, ...) could be detected in both reductant and oxidants steps. Results show that the reactivity of the carrier is not significantly affected by the presence of methane. Actually, performances are slightly better. Initial conversions of H₂S are similar at both temperatures but appear more stable in presence of methane. Selectivity to SO₂ formation is also slightly lower in both reductant and oxidant steps in presence of methane. Considering that a fresh carrier sample was used for these experiments and the inherent experimental margins, it is hazardous to attribute the better performances to the presence of methane. Most important is that very similar trends can be observed, in particular in terms of selectivity.

Reactivity of methane alone over was tested in a similar cycling mode up to 500 °C. No measurable methane conversion could be observed within experimental error (i.e. $\text{Conv}_{\text{CH}_4} < 1\%$) in the full temperature range explored (150-500 °C). Some traces of CO and CO₂ production could be detected only at the highest temperature. This means that in the temperature range of interest for H₂S selective oxidation (150-250 °C), methane is unreactive. This confirms that the preferential oxidation of the H₂S in the presence of methane can be performed.

4. Characterization of carriers before and after reduction and oxidation steps

The specific surface area of V₂O₅ before chemical looping reaction is of 5.5 m² gr⁻¹. It could not be measured after reaction due to the low amount of carrier used in experiments.

Samples were studied before and after reaction to evaluate the structural or chemical changes in the catalysts during the reaction. Two samples were considered by ending either after the reductant or the oxidant steps.

Different samples were submitted to CL at two temperatures (150°C and 200 °C) using 2000 ppm of H₂S with 10000 ppm of O₂. CL cycles were performed on all samples and the reaction was stopped after the 30th cycle either after the H₂S step or after O₂ step. The reactor was then closed and cooled to room temperature. So, in total 4 samples were obtained after CL reaction:

V₂O₅ (H₂S, 150 °C): reaction stopped after the H₂S step at 150 °C.

V₂O₅ (H₂S, 200 °C): reaction stopped after the H₂S cycle at 200 °C.

V₂O₅ (O₂, 150 °C): reaction stopped after the O₂ cycle at 150 °C.

V₂O₅ (O₂, 200 °C): reaction stopped after the O₂ cycle at 200 °C.

4.1. XRD

Before reaction, X-ray diffraction patterns of bulk V₂O₅ shows (Figure 10) the presence of the crystalline phase of V₂O₅. Orthorhombic lattice is observed for the V₂O₅ with an intense peak at $2\theta = 20.26$. The intense peak represents the typical plane of (1 0 1) (JCPDF file 00-041-1426). The average crystallite size determined by XRD is 86 nm.

Figure 10. XRD of bulk V₂O₅ before and after chemical looping: (•) V₂O₅, (◊) VO₂, (↓) V₄O₅

A: overall diffractogram; B: detail

A small supplementary peak at $2\theta=27.7^\circ$ can be observed and could be attributed to VO₂ (0 1 0) plane, according to JCPDF file 04-003-2035. This peak is present at various intensities on all samples after reaction and more intensely on samples collected after reaction at 200 °C.

Samples collected after reaction at 200 °C after both reductant and oxidant steps show small peaks at $2\theta = 13.7, 21.3, 21.7, 28.1$ which could indicate the presence of V₄O₉, [26-28] with reference to the JCPDF file 23-720. However, the small peak at $2\theta=21.3^\circ$ could also be attributed to elemental sulfur, plane (0 2 0), in reference to the JCPDF file 01-076-1100. The presence of crystalized S particles would nevertheless be rather surprising on samples collected at higher temperature and not on those collected at 150 °C as the risk of sulfur condensation and accumulation increases at lower temperature.

4.2. XPS

Before reaction, XPS spectrum of V_2O_5 (Figure 11) is characterized by two photopeaks at V $2p_{3/2}$ and V $2p_{1/2}$ with ΔE 7.6 eV. The chemical shift observed on the photopeak V $2p_{3/2}$ is used to distinguish the V^{4+} and V^{5+} species when the vanadium is found in two distinct phases and two different degrees of oxidation. ΔE between the O 1s and V $2P_{3/2}$ is 12.9 eV, confirming the presence of V^{5+} oxidation state in the solid [29]. For deconvolution of V $2P_{3/2}$, the presence of V^{5+} species at 517.5 eV and V^{4+} at 516 eV are considered [30-32].

Both V^{4+} and V^{5+} are observed throughout the study. By the deconvolution of the different components, it is possible to estimate the ratios of V^{4+}/V^{5+} , which are reported in Table 4.

Contrary to what could be expected, no significant differences in the V^{4+}/V^{5+} ratio can be observed on the samples although they were collected at different temperatures and after reductant or oxidant steps.

Figure 11. XPS study of V_2O_5 before and after reaction (V2p and O1s)

Table 4. XPS analysis of samples before and after reaction, distribution of V^{4+} and V^{5+} species.

This could be explained by the fact that once the step is performed and the reactor closed, the surface oxidation state may evolve thanks to oxygen diffusion between the bulk of the solid and its surface. What seems more significant is that even after the oxidant step, V^{4+}

species are present. This would indicate that the full oxidation to V^{5+} does not occur even at the highest temperature.

For oxygen, the O 1s signal clearly shows three different surface oxygen species. As explained by Cornaglia et al. [31] and et al. Biesinger [33] photopeak at 530.59 eV represents the oxygen associated with the Vanadium species, the one at 530.11 eV represents the mobile oxygen in the solid and photo peak at 531.79 eV corresponds to adsorbed oxygen, hydroxyl and/or carbonate groups.

Figure 12. XPS study of V_2O_5 before and after reaction (S 2p)

Practically no sulfur can be detected on these samples (Figure 12), with the exception of the sample collected after the reductant step at 150 °C. In this case, a peak at 168.8 eV is seen, providing a S/V ratio of approx. 0.02. From the position of the S2p peak, sulfate formation on the surface of V_2O_5 cannot be excluded [34].

The absence of S on the sample treated at 200 °C is also surprising considering that SO_2 is produced during the oxidant step in these conditions. To allow this to happen, sulfur containing species must be present in the adsorbed form on the surface after the reductant step. Again, the diffusion of oxygen from the bulk, which is enhanced by temperature, could explain that these adsorbed species continue to be oxidized by the carrier during the period the reactor is closed before cooling to room temperature.

4.3. Raman

The Raman spectrum of V_2O_5 before and after CL reaction is shown in Figure 13. For the original carrier, the narrow peak at 997 cm^{-1} , due to the symmetric stretching vibrations of V-O groups, is characteristic of crystalline V_2O_5 . Additional bands observed near 704 cm^{-1} arise from the stretching vibrations of V-O in the square octahedron of V_2O_5 . The peaks at 146, 289, 304, 488, 704, and 997 cm^{-1} are attributable to different crystalline V_2O_5 species [27,19].

Figure 13 . Raman study of V_2O_5 before and after the reaction

After reaction, all the peaks of the bulk V_2O_5 are present at both the temperatures or at the last exposed reactant. However, after reaction at $200\text{ }^\circ\text{C}$, a small shoulder at 903 cm^{-1} is observed irrespective of the last reactant present. As shown by Luan et al. [35], this peak can be assigned to bridge V-O-V chain vibrations of polymeric vanadium oxide species as these peaks feature in the $800\text{-}900\text{ cm}^{-1}$ region. The peak at 903 cm^{-1} could also show the presence of $V^{5+}\text{-O-V}^{4+}$ from V_4O_9 structure, as shown by Nieto et al. [26,27] .

5. Discussion

Bulk V_2O_5 shows interesting activity for chemical looping oxidation of H_2S at low the temperature range of $150\text{ to }200\text{ }^\circ\text{C}$. Experiments performed with 20, or in some case, 30, cycles show that a “steady” repetitive behavior is not always reached both in terms of H_2S

conversion and selectivity to SO_2 in reductant and oxidant steps. Important trends can nevertheless be found which will allow to optimize the system.

In comparison to co-feed reactions, rather similar overall performances are observed in terms of stability (20 cycles would correspond to 20 reaction in H_2S). In terms of selectivity, the overall SO_2 production is also rather similar. The most striking difference is that the SO_2 production during reductant step in CL is usually low and that in all cases the SO_2 formation occurs mostly during oxidant step due to excessive unreacted sulfur species remaining adsorbed after reductant step. This confirms the potential of chemical looping process to achieve better selectivity towards elemental sulfur by decoupling the two steps of reaction and avoiding direct contact between H_2S and O_2 . However, it also illustrates the need for further optimization of CL operating conditions to avoid excess H_2S adsorption with respect to the oxidation capacity of the carrier.

The conversion of the H_2S varies with temperature and with different concentrations of the reactant. Considering that one V_2O_5 unit will occupy approx. 0.21 nm^2 [36], taking into account the specific surface area of the solid ($5.5 \text{ m}^2 \text{ gr}^{-1}$) and the amount used (80 mg), the amount of surface V_2O_5 can be estimated to approx. $0.6 \text{ } \mu\text{mol}$ for these experiments, to be compared to $440 \text{ } \mu\text{mol}$ of total V_2O_5 . As seen in Table 3, the percentage of lattice oxygen involved varies between 0.9 and 2.2 % O_{latt} , i.e. between 4 and 16 μmol , which would represent the involvement of 6 to 16 layers of V_2O_5 . This is obtained considering exclusively the reduction of V^{5+} species to V^{4+} and the numbers of layers involved would clearly be smaller if a reduction to V^{3+} takes place. In any case, this indicates that both surface species and subsurface layers of the oxide are involved to account for the reactivity of the system.

It was observed that in all cases, some SO₂ is formed during the reductant step. The amount (SO₂R) varies from 0.1 to 1.1 μmol (Table 3) according to reaction conditions. These values are in the same order of magnitude as that of surface V₂O₅ calculated above and could suggest that the outermost oxidized vanadium species generated during the re-oxidation result in unselective oxidation. However, in this case, this amount should not vary significantly. On the contrary, as seen, the amount of SO₂R increases significantly with temperature and is also affected by the concentration of H₂S, in particular at 150 °C.

Another way to explain this is that certain surface planes exposed by the solid lead to unselective oxidation, which can then proceed more deeply through subsurface layers according to temperature and H₂S pressure, while other planes would show better selectivity. This anisotropic behavior of crystalline oxides has already been observed for several selective oxidation reactions [37,38].

The contribution of deep subsurface layers of the oxide is coherent with the presence of both V⁴⁺ and V⁵⁺ species on all samples after the experiment, independently of reaction temperature and of the nature of the last step before recovering the sample. If the presence of V⁴⁺ species could be expected after the reductant step, it was more surprising after the oxidant one. However, if one considers that the subsurface layers are progressively involved during cycling, it is possible that the re-oxidation does not proceed so deeply at each cycle. If reduced species are still present, the solid would slowly re-equilibrate by diffusion of oxygen species from surface towards the bulk. Inversely, deeper oxygen species from the bulk may migrate to the subsurface in samples recovered after the reductant step.

On the other hand, XRD and Raman show the formation of V_4O_9 phase on samples tested at 200°C . This phase is observed on samples collected after both reductant and oxidant steps. This indicates a structural modification of the sample during cycling which seems to be favored by higher temperature and thus mobility of oxygen species in the solid. This V_4O_9 phase has been observed and identified as responsible for selective oxidation of H_2S in co-feed conditions [26]. One could therefore suppose that the solid is progressively reduced from V_2O_5 to V_4O_9 during cycling. At this point, the carrier phase would retain a good selectivity to oxidize H_2S to S in reductant step generating low amounts of SO_2 in this step. However, by reducing the amount of V^{5+} species available to perform such oxidation, thus reducing the oxygen capacity of the carrier, more adsorbed species remain unreacted at the end of reductant step and are subsequently oxidized to SO_2 in oxidant step.

This result shows that the transient nature of the process must always be considered when comparing results considering that the solid continues to evolve between reaction steps, where it is submitted to external “stress”, and relaxation periods.

This could also be featured regarding the presence of sulfur species on samples after the test. No S could be detected by XPS even on sample treated at 200°C after H_2S exposure. Although S should be present after such cycling, its absence during characterization suggests that it continues to be converted by the solid.

Finally, the preferential oxidation of H_2S in the presence of methane is confirmed in line with results obtained by Palma et al [5] on ceria supported vanadium oxide catalyst for abatement of H_2S from biogas at low temperature. They achieved preferential oxidation of H_2S in presence of methane and carbon dioxide with no byproducts such as COS_2 , CS_2 observed

during the reaction. The major difference is that O_2 needed to be co-fed with the biogas which involve serious safety limitations for practical development at large scale. In this respect, chemical looping offers the advantage of avoiding dangerous mixtures.

The absence of reactivity of methane in these conditions is not a surprise as for most catalytic reaction using oxide-based catalysts, much higher reaction temperatures are needed. For example, in the case of V based catalysts, temperature between 550 and 650 °C had to be used for the oxidation of methane to formaldehyde on silica supported V as shown by Loricera et al.[39] or Nguyen et al.[40].

6. Conclusions

The concept of chemical looping was implemented for the first time for selective oxidation of H_2S . The results confirm that V_2O_5 is a potential candidate as an active phase in oxygen carriers for this reaction. They show that H_2S can be selectively converted to elemental S on such materials, which further demonstrate to have interesting cyclic regeneration properties both in terms of oxygen capacity and surface sulfur species removal.

It can be confirmed that not only outermost surface species are involved in the redox process. Indeed, rather deep reduction/oxidation of the solid is possible even at such low reaction temperature and the formation of V_4O_9 phase appears to be significant in determining the performances of the carrier. However, the transient nature of chemical looping processes makes a further hypothesis on the reaction mechanism highly hypothetical at this point.

In most conditions explored, selectivity to elemental sulfur is high, although some SO_2 is formed during the reductant cycle. Actually, most of the SO_2 is produced during the oxidant

step. This confirms the interest for decoupling the two reaction steps by chemical looping. However, improvements remain to be done to enhance the reactivity of the active phase in order to limit the presence of unreacted or partially unreacted species adsorbed during the reductant step. Another crucial aspect is the stability of the performances along cycling which needs to be achieved either by the design of better carriers or by optimizing the operating conditions.

In line with the well-known activity of V_2O_5 in co-feed selective oxidation of H_2S and with the thermodynamic considerations, these results confirm that vanadium oxide materials can effectively be considered as active carriers in such novel chemical looping process and which allows having selective and preferential oxidation of H_2S to S.

Acknowledgments

The Fonds Européen de Développement Régional (FEDER), CNRS, Région Hauts-de-France and Ministère de l'Éducation Nationale de l'Enseignement Supérieur et de la Recherche are acknowledged for funding of XPS spectrometers within the Pôle Régional d'Analyses de Surface and XRD instruments. TK and JGC are grateful to Univ. Lille and Région Hauts-de-France for providing financial support.

References

[1] A. Piéplu, O. Saur, J.C. Lavalley, O. Legendre, C. Nédez, Claus catalysis and H_2S selective oxidation, *Catalysis Reviews* 40 (1998) 409-450 doi:10.1080/01614949808007113.

- [2] P. Kalinkin, O. Kovalenko, O. Lapina, D. Khabibulin, N. Kundo, Kinetic peculiarities in the low-temperature oxidation of H₂S over vanadium catalysts, *J. Mol. Catal. A Chem.* 178 (2002) 173–180. doi:10.1016/S1381-1169(01)00292-8.
- [3] Y.G. Cho, H.C. Woo, J.S. Chung, Selective oxidation of hydrogen sulfide to ammonium thiosulfate and sulfur over vanadium-bismuth oxide catalysts, *Res. Chem. Intermed.* 28 (2002) 419–431. doi:10.1163/156856702760346833.
- [4] J. Kijenski, A. Baiker, M. Glinski, P. Dollenmeier, A. Wokaun, Monolayers and double layers of vanadium pentoxide on different carriers: Preparation, characterization and catalytic activities, *J. Catal.* 101 (1986) 1–11. doi:10.1016/0021-9517(86)90222-8.
- [5] V. Palma, D. Barba, Vanadium-ceria catalysts for H₂S abatement from biogas to feed to MCFC, *Int. J. Hydrogen Energy.* 42 (2017) 1891–1898. doi:10.1016/j.ijhydene.2016.06.160.
- [6] A. Corma, H. García, Lewis acids as catalysts in oxidation reactions: From homogeneous to heterogeneous systems, *Chem. Rev.* 102 (2002) 3837–3892. doi:10.1021/cr010333u.
- [7] A.A. Davydov, V.I. Marshneva, M.L. Shepotko, Metal oxides in hydrogen sulfide oxidation by oxygen and sulfur dioxide: I. The comparison study of the catalytic activity. Mechanism of the interactions between H₂S and SO₂ on some oxides, *Appl. Catal. A Gen.* 244 (2003) 93–100. doi:10.1016/S0926-860X(02)00573-2.
- [8] B. Pongthawornsakun, S. Phatyenchen, J. Panpranot, P. Praserttham, The low temperature selective oxidation of H₂S to elemental sulfur on TiO₂ supported V₂O₅ catalysts, *J. Environ. Chem. Eng.* 6 (2018) 1414–1423. doi:10.1016/j.jece.2018.01.045.

- [9] I.E. Wachs, R.Y. Saleh, S.S. Chan, C.C. Chersich, The interaction of vanadium pentoxide with titania (anatase): Part I. Effect on o-xylene oxidation to phthalic anhydride, *Appl. Catal.* 15 (1985) 339–352. doi:10.1016/S0166-9834(00)81848-5.
- [10] T. Machej, J. Haber, A. M. Turek, I. E. Wachs, Monolayer V_2O_5/TiO_2 and MoO_3/TiO_2 catalysts prepared by different methods, *Appl. Catal.* 70 (1991) 115–128. doi:10.1016/S0166-9834(00)84158-5.
- [11] D.W. Park, B.K. Park, D.K. Park, H.C. Woo, Vanadium-antimony mixed oxide catalysts for the selective oxidation of H_2S containing excess water and ammonia, *Appl. Catal. A Gen.* 223 (2002) 215–224. doi:10.1016/S0926-860X(01)00760-8.
- [12] I.E. Wachs, B.M. Weckhuysen, Structure and reactivity of surface vanadium oxide species on oxide supports, *Appl. Catal. A Gen.* 157 (1997) 67–90. doi:10.1016/S0926-860X(97)00021-5.
- [13] V. Palma, D. Barba, Low temperature catalytic oxidation of H_2S over V_2O_5/CeO_2 catalysts, *Int. J. Hydrogen Energy.* 39 (2014) 21524–21530. doi:10.1016/j.ijhydene.2014.09.120.
- [14] M.Y. Shin, D.W. Park, J.S. Chung, Vanadium-containing catalysts for the selective oxidation of H_2S to elemental sulfur in the presence of excess water, *Catal. Today.* 63 (2000) 405–411. doi:10.1016/S0920-5861(00)00485-5.
- [15] T. Mattisson, Martin Keller, C. Linderholm, P. Moldenhauer, M. Ryden, H. Leion, A. Lyngfelt, Chemical-looping technologies using circulating fluidized bed systems: Status of development, *Fuel Process. Technol.* 172 (2018) 1–12. doi:10.1016/j.fuproc.2017.11.016.

- [16] Z. Guo, B. Liu, Q. Zhang, W. Deng, Y. Wang, Y. Yang, Recent advances in heterogeneous selective oxidation catalysis for sustainable chemistry, *Chem. Soc. Rev.* 43 (2014) 3480–3524. doi:10.1039/C3CS60282F.
- [17] A. Corma, L. Sauvanaud, FCC testing at bench scale: New units , new processes , new feeds, *Catal. Today.* 218–219 (2013) 107–114. doi:10.1016/j.cattod.2013.03.038.
- [18] J. Herguido, M. Mene, J. Santamarı, Oxidative Dehydrogenation of n -Butane in a Two-Zone Fluidized-Bed Reactor, *Ind. Eng. Chem. Res.* 38 (1999) 90–97 doi:10.1021/ie980486g
- [19] A. Löfberg, J. Guerrero-Caballero, T. Kane, A. Rubbens, L. Jalowiecki-Duhamel, Ni/CeO₂ based catalysts as oxygen vectors for the chemical looping dry reforming of methane for syngas production, *Appl. Catal. B Environ.* 212 (2017) 159–174. doi:10.1016/j.apcatb.2017.04.048.
- [20] S. Bhavsar, M. Najera, G. Veser, Chemical Looping Dry Reforming as Novel, Intensified Process for CO₂ Activation, *Chem. Eng. Technol.* 35,7 (2012) 1281–1290. doi:10.1002/ceat.201100649.
- [21] J. Ma, C. Wang, H. Zhao, X. Tian, Sulfur fate during lignite pyrolysis process in chemical looping combustion environment, *Energy & Fuels.* 32 (2018) 4493–4501. doi:10.1021/acs.energyfuels.7b03149.
- [22] R.F. Pachler, K. Mayer, S. Penthor, M. Kollerits, H. Hofbauer, Fate of sulfur in chemical looping combustion of gaseous fuels using a copper-based oxygen carrier, *Int. J. Greenh. Gas Control.* 71 (2018) 86–94. doi:10.1016/j.ijggc.2018.02.006.

- [23] M. Young, C. Mo, D. Won, J. Shik, Selective oxidation of H₂S to elemental sulfur over VO_x/SiO₂ and V₂O₅ catalysts, *Appl. Catal. A Gen.* 211 (2001) 213–225. doi:10.1016/S0926-860X(00)00866-8.
- [24] S. Besselmann, C. Freitag, O. Hinrichsen, M. Muhler, Temperature-programmed reduction and oxidation experiments with V₂O₅/TiO₂ catalysts, *Phys. Chem. Chem. Phys.* 3 (2001) 4633–4638. doi:10.1039/b105466j.
- [25] C.W. Bale, E. Bélisle, P. Chartrand, S.A. Deckerov, G. Eriksson, K. Hack, I.H. Jung, Y.B. Kang, J. Melançon, A.D. Pelton, C. Robelin, S. Petersen, FactSage thermochemical software and databases - recent developments, *Calphad Comput. Coupling Phase Diagrams Thermochem.* 33 (2009) 295–311. doi:10.1016/j.calphad.2008.09.009. <www.factsage.com>
- [26] J.P. Holgado, M.D. Soriano, J. Jiménez-Jiménez, P. Concepción, A. Jiménez-López, A. Caballero, E. Rodríguez-Castellón, J.M.L. Nieto, Operando XAS and Raman study on the structure of a supported vanadium oxide catalyst during the oxidation of H₂S to sulphur, *Catal. Today.* 155 (2010) 296–301. doi:10.1016/j.cattod.2010.02.050.
- [27] M.D. Soriano, J. Jiménez-Jiménez, P. Concepción, A. Jiménez-López, E. Rodríguez-Castellón, J.M.L. Nieto, Selective oxidation of H₂S to sulfur over vanadia supported on mesoporous zirconium phosphate heterostructure, *Appl. Catal. B Environ.* 92 (2009) 271–279. doi:10.1016/j.apcatb.2009.08.002.
- [28] R. Nilsson, T. Lindblad, A. Andersson, Ammoxidation of propene over antimony-vanadium-oxide catalysts, *Catal. Letters.* 29 (1994) 409–420. doi:10.1007/BF00807120.
- [29] S. Surnev, M.G. Ramsey, F.P. Netzer, Vanadium oxide surface studies, *Prog. Surf. Sci.* 73 (2003) 117–165. doi:10.1016/j.progsurf.2003.09.001.

- [30] G.C. Bond, S.F. Tahir, Vanadium oxide monolayer catalysts Preparation, characterization and catalytic activity, *Appl. Catal.* 71 (1991) 1–31. doi:10.1016/0166-9834(91)85002-D.
- [31] L.M. Cornaglia, E.A. Lombardo, XPS studies of the surface oxidation states on equilibrated catalysts, *Appl. Catal. A.* 127 (1995) 125–138. doi:10.1016/0926-860X(95)00067-4
- [32] J. Mendialdua, R. Casanova, Y. Barbaux, XPS studies of V_2O_5 , V_6O_{13} , VO_2 and V_2O_3 , *J. Electron Spectros. Relat. Phenomena.* 71 (1995) 249–261. doi:10.1016/0368-2048(94)02291-7.
- [33] M.C. Biesinger, L.W.M. Lau, A.R. Gerson, R.S.C. Smart, Resolving surface chemical states in XPS analysis of first row transition metals, oxides and hydroxides: Sc, Ti, V, Cu and Zn, *Appl. Surf. Sci.* 257 (2010) 887–898. doi:10.1016/j.apsusc.2010.07.086.
- [34] B. Barbaray, J.P. Contour, G. Mouvier, Sulfur Dioxide Oxidation Over Atmospheric Photoelectron Spectra of Sulfur Dioxide Adsorbed on V_2O_5 and Carbon, *Atmos. Environ.* 11 (1977) 351–356. doi:10.1016/0004-6981(77)90163-9
- [35] Z. Luan, P.A. Meloni, R.S. Czernuszewicz, L. Kevan, Raman spectroscopy of vanadium oxide species immobilized at surface titanium centers of mesoporous titanosilicate TiMCM-41 molecular sieves, *J. Phys. Chem. B.* 101 (1997) 9046–9051. doi:10.1021/jp971613
- [36] F. Roozeboom, T. Fransen, P. Mars, P.J. Gellings, Vanadium oxide monolayer catalysts. I. Preparation, characterization, and thermal stability, *ZAAC - J. Inorg. Gen. Chem.* 449 (1979) 25–40. doi:10.1002/zaac.19794490102.
- [37] J.M. López Nieto, B. Solsona, Gas phase heterogeneous partial oxidation reactions, in: *Met. Oxides Heterog. Catal.*, 2018: pp. 211–286. doi:10.1016/b978-0-12-811631-9.00005-3.

- [38] A.W. Potts, G.R. Morrison, L. Gregoratti, S. Gunther, M. Kiskinova, M. Marsi, Selective oxidation of surface grains in polycrystalline tin, *Chem. Phys. Lett.* 290 (1998) 304–310. doi:10.1016/S0009-2614(98)00523-5.
- [39] C. V. Loricera, M.C. Alvarez-Galvan, R. Guil-Lopez, A.A. Ismail, S.A. Al-Sayari, J.L.G. Fierro, Structure and Reactivity of sol–gel V/SiO₂Catalysts for the Direct Conversion of Methane to Formaldehyde, *Top. Catal.* 60 (2017) 1129–1139. doi:10.1007/s11244-017-0809-x.
- [40] L.D. Nguyen, S. Loridant, H. Launay, A. Pigamo, J.L. Dubois, J.M.M. Millet, Study of new catalysts based on vanadium oxide supported on mesoporous silica for the partial oxidation of methane to formaldehyde: Catalytic properties and reaction mechanism, *J. Catal.* 237 (2006) 38–48. doi:10.1016/j.jcat.2005.10.016.

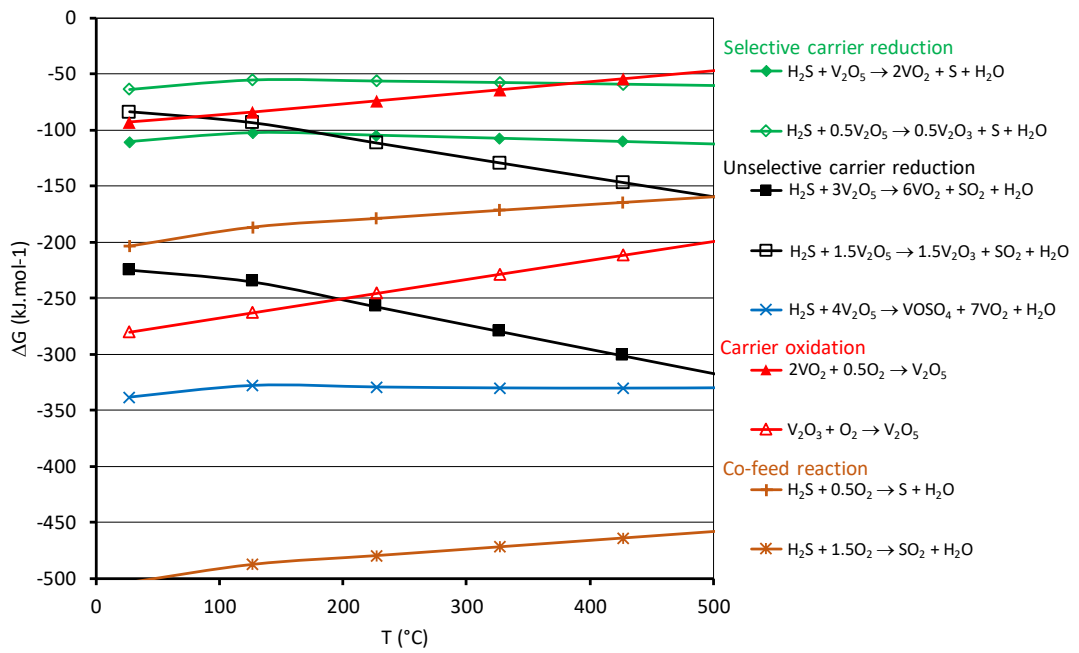


Figure 1: Variation of standard Gibbs free energy with temperature for H_2S oxidation by V_2O_5 .

Reduction of V_2O_5 by H_2S to VO_2 (closed symbols) or V_2O_3 (open symbols), selective oxidation to S (green), unselective to SO_2 (black), carrier re-oxidation by O_2 (red), co-feed reaction in brown with $\text{H}_2\text{S}:\text{O}_2 = 1:5$ and $1:0.5$ (brown), VOSO_4 formation (blue)

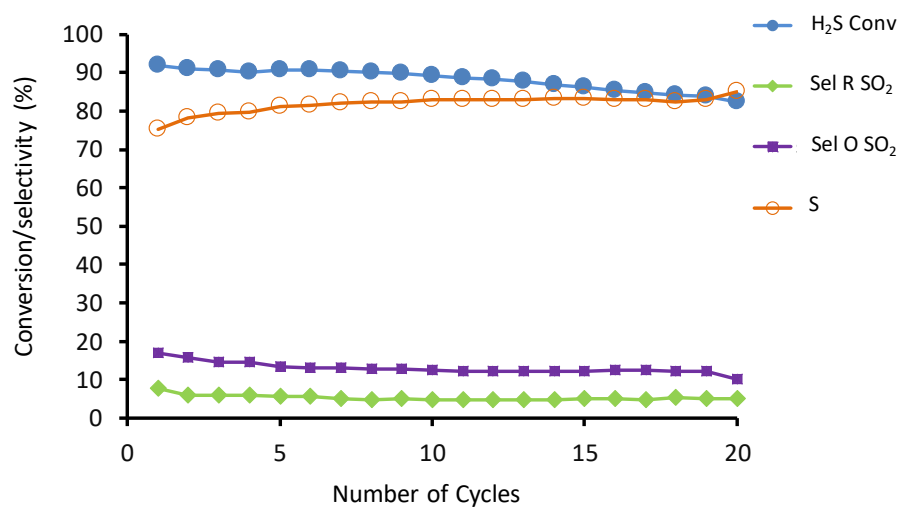


Figure 2. Chemical looping oxidation of H₂S; 80 mg V₂O₅ + 900 mg SiC at 150 °C, F_T = 100 mL min⁻¹,
 Cycle: 1 min. in 2000 ppm of H₂S, and 1 min. in O₂ of 10000 ppm of O₂ (H₂S:O₂ = 1:5)

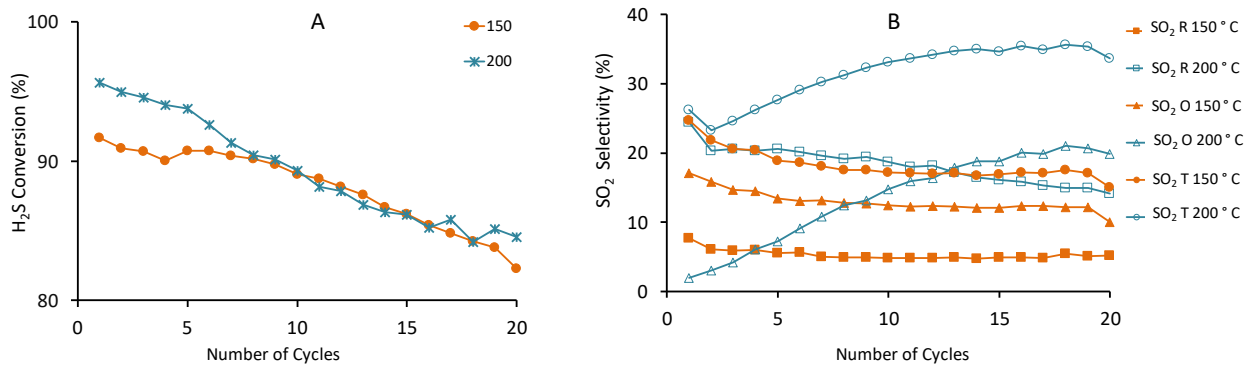


Figure 3. Chemical looping oxidation of H₂S; 80 mg V₂O₅ + 900 mg SiC at 150 °C, F_T = 100 mL min⁻¹,

Cycling: 1 min. in 2000 ppm of H₂S, and 1 min. in O₂ of 10000 ppm of O₂ (H₂S:O₂ = 1:5)

A: H₂S conversion, B: SO₂ selectivity (in reductant steps, oxidant steps and overall)

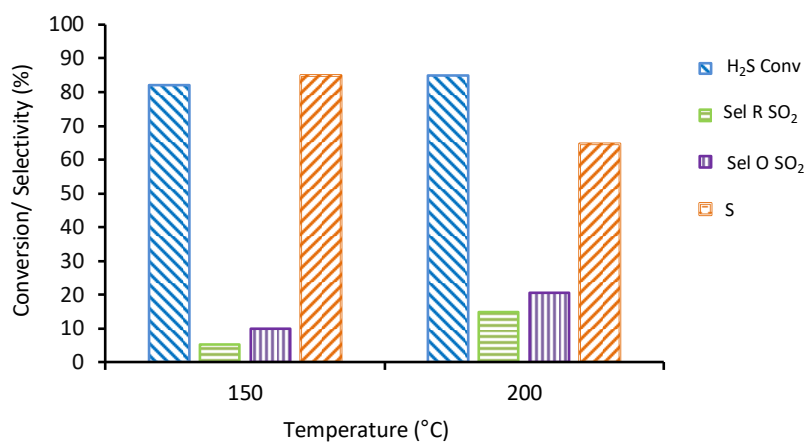


Figure 4. Chemical looping oxidation of H₂S, overall performance at 20 cycles; 80 mg V₂O₅ + 900 mg SiC at 150 °C, F_T = 100 mL min⁻¹; Cycling: 1 min. in 2000 ppm of H₂S, and 1 min. in O₂ of 10000 ppm of O₂ (H₂S:O₂ = 1:5)

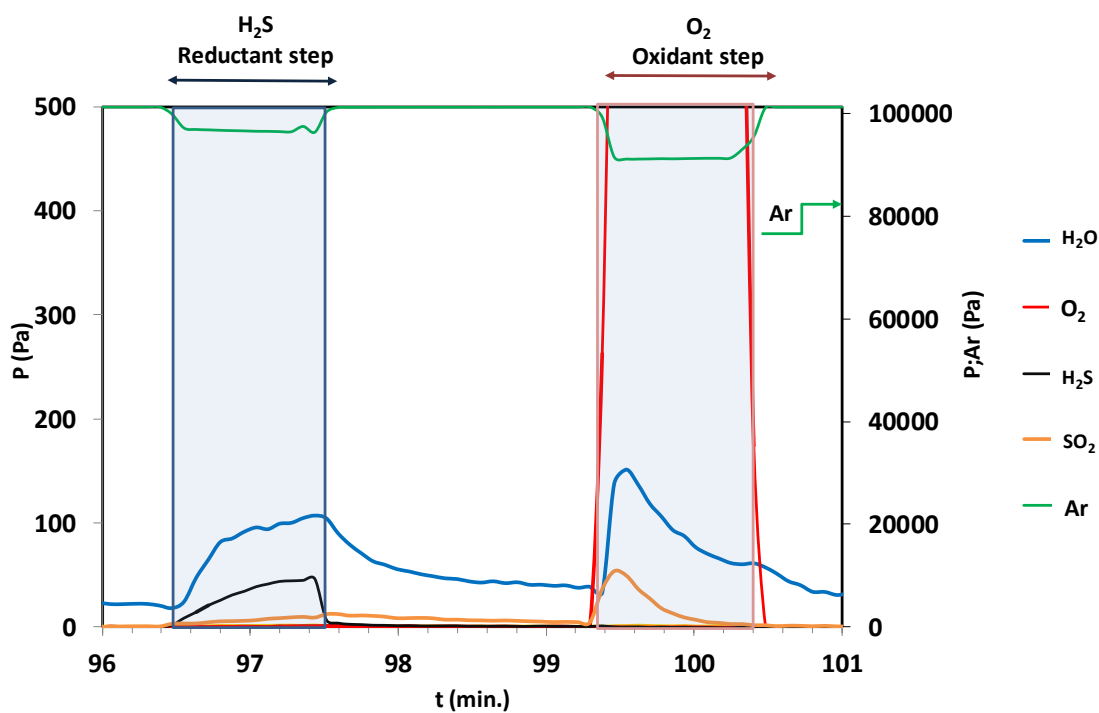
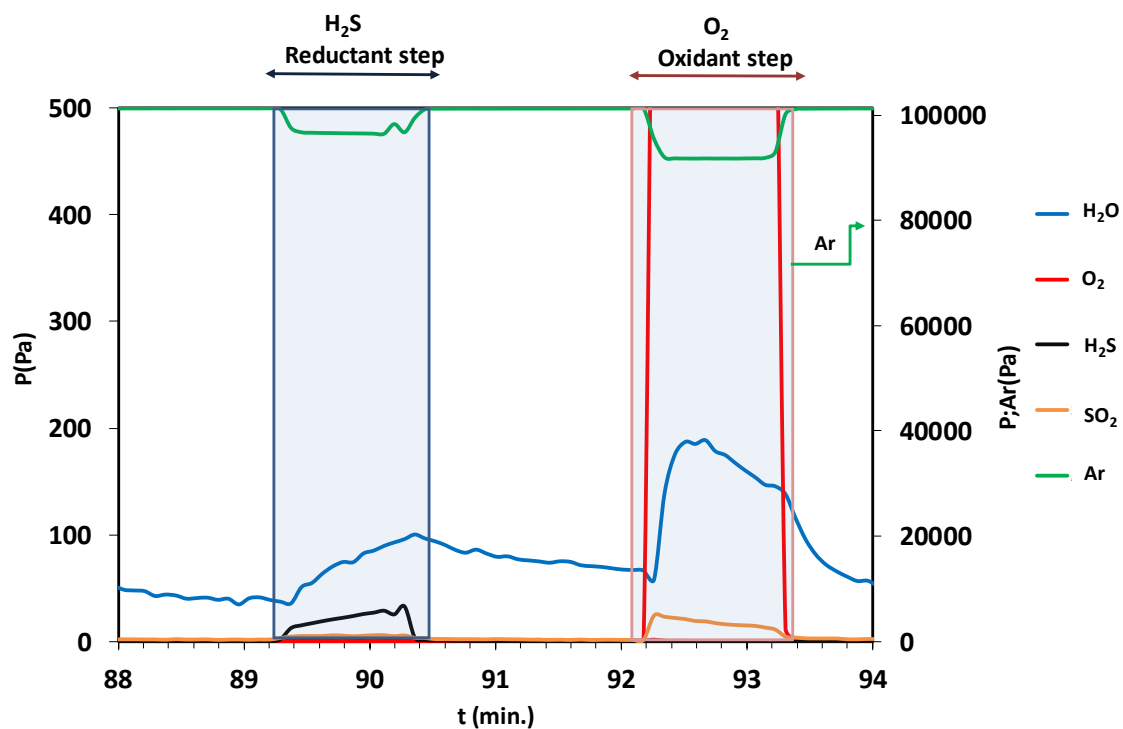
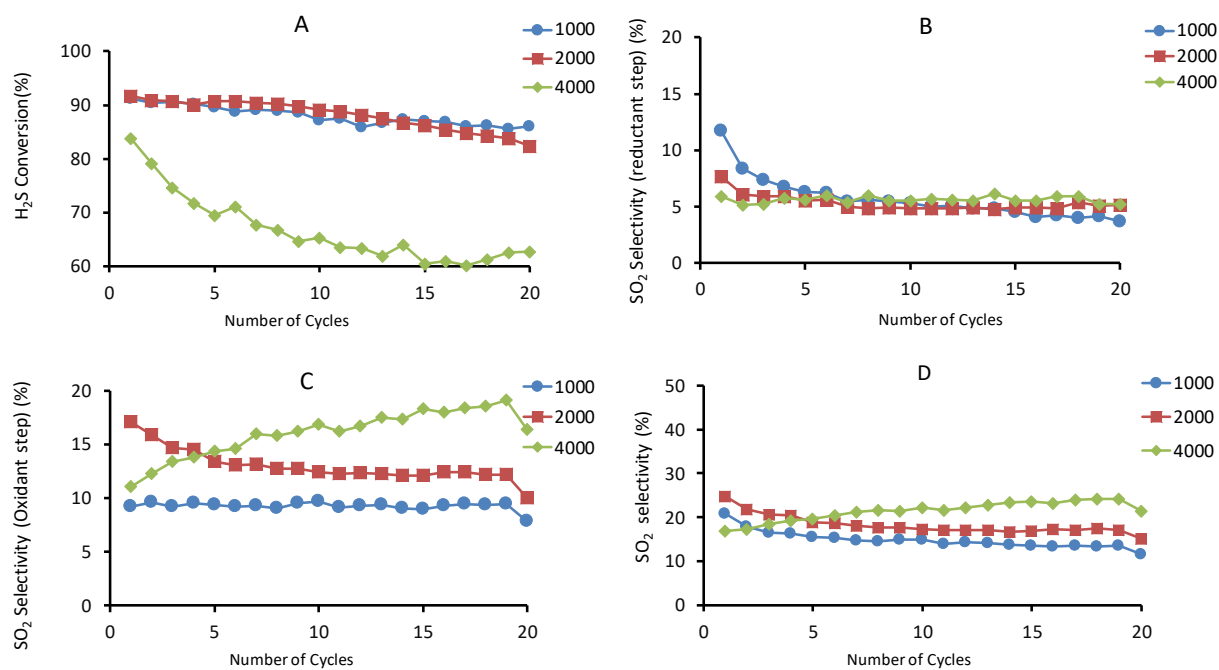


Figure 5. Detailed gas evolution during cycling; 80 mg V_2O_5 + 900 mg SiC at 150 °C, $F_T = 100 \text{ mL min}^{-1}$;

Cycling: 1 min. in 2000 ppm of H_2S , and 1 min. in O_2 of 10000 ppm of O_2 ($H_2S:O_2 = 1:5$)

A: 150°C and B: 200°C



Figures 6. Chemical looping oxidation of H₂S with different H₂S-O₂ concentrations; 80 mg V₂O₅ + 900 mg SiC at 150°C, F_T = 100 mL min⁻¹; Cycling: 1 min. in H₂S (4000, 2000, 1000 ppm) and 1 min. in O₂ (H₂S:O = 1:5)

A: H₂S conversion, B: SO₂ selectivity in reductant step, C: SO₂ selectivity in oxidant step, D: overall SO₂ selectivity

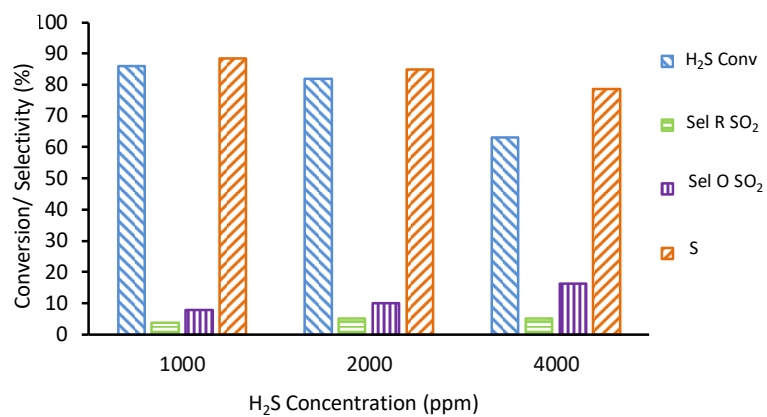


Figure 7. Overall performances during last cycle (20th) with different H₂S-O₂ concentrations; 80 mg

V₂O₅ + 900 mg SiC at 150°C, F_T = 100 mL min⁻¹;

Cycling: 1 min. in H₂S (4000, 2000, 1000 ppm) and 1 min. in O₂ (H₂S:O₂ = 1:5)

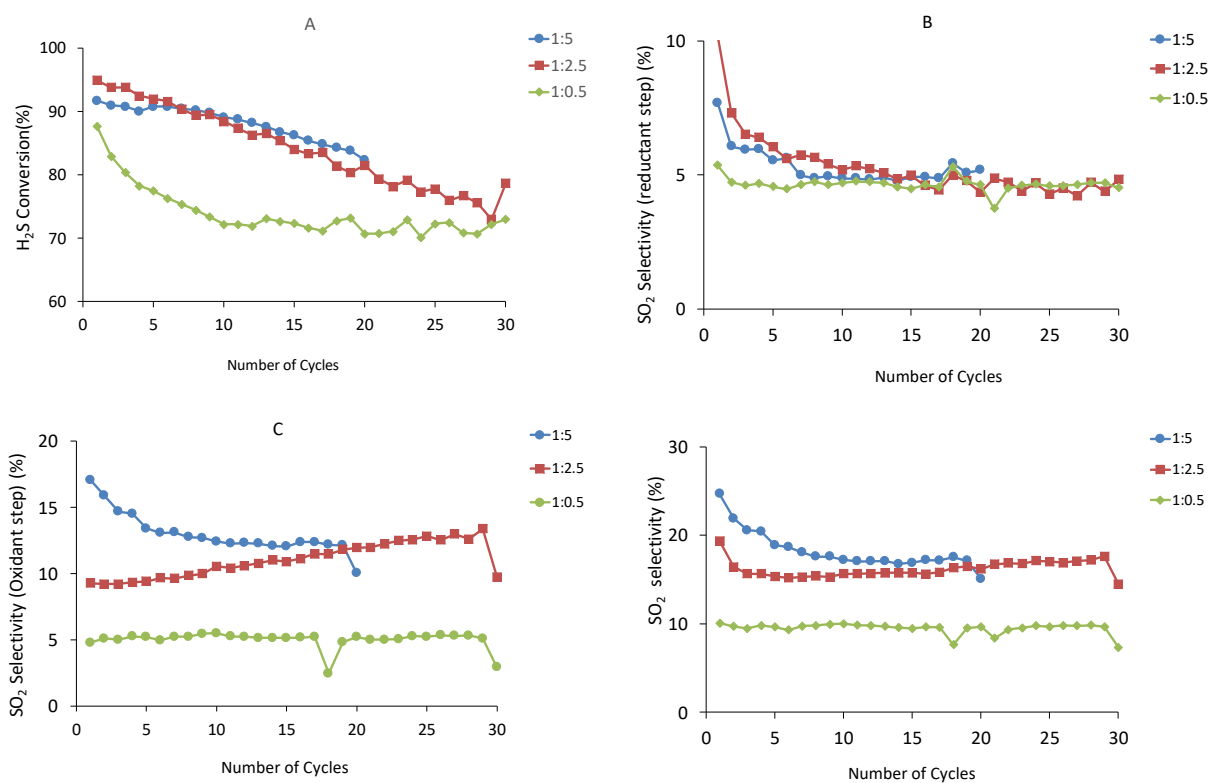


Figure 8. Chemical looping oxidation of H_2S with different $H_2S:O_2$ ratio, 80 mg V_2O_5 + 900 mg SiC at $150^\circ C$, $F_T = 100 \text{ mL min}^{-1}$, Cycling: 1min. in 2000 ppm of H_2S , and 1 min. in O_2 ; $H_2S:O_2 = 1:5, 1:2.5, 1:0.5$

A: H_2S conversion, B: SO_2 selectivity in reductant step, C: SO_2 selectivity in oxidant step, D: overall SO_2 selectivity

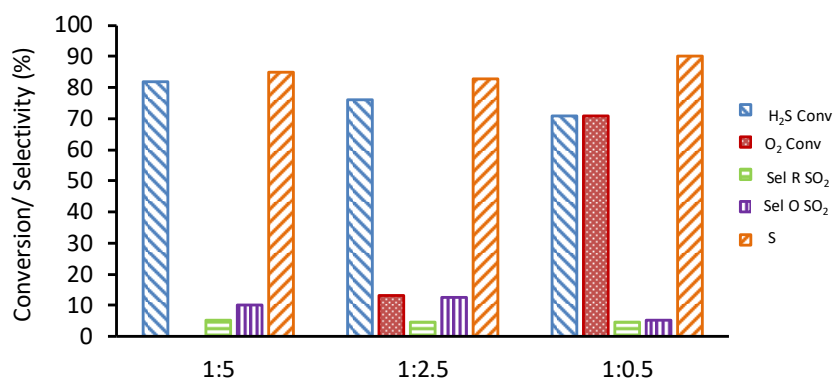


Figure 9. Overall performances during last cycle with different H₂S:O₂ ratio; 80 mg V₂O₅ + 900 mg SiC at 150°C, F_T = 100 mL min⁻¹, Cycle: 1min. in 2000 ppm of H₂S, and 1 min. in O₂; H₂S:O₂ = 1:5 (20th cycle), 1:2.5 (30th cycle), 1:0.5 (30th cycle)

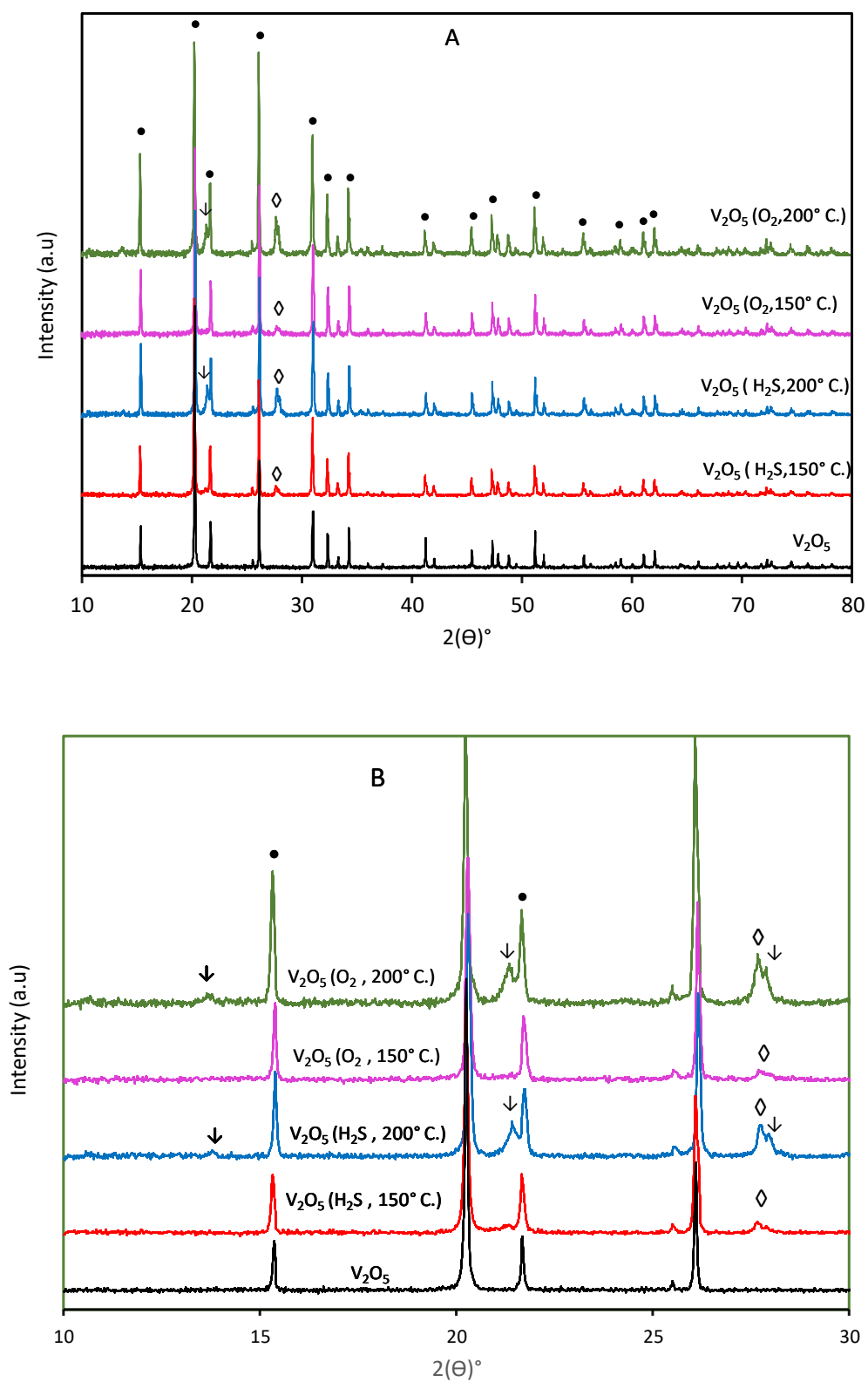


Figure 10. XRD of bulk V_2O_5 before and after chemical looping: (•) V_2O_5 , (◊) VO_2 , (↓) V_4O_5
 A: overall diffractogram; B: detail

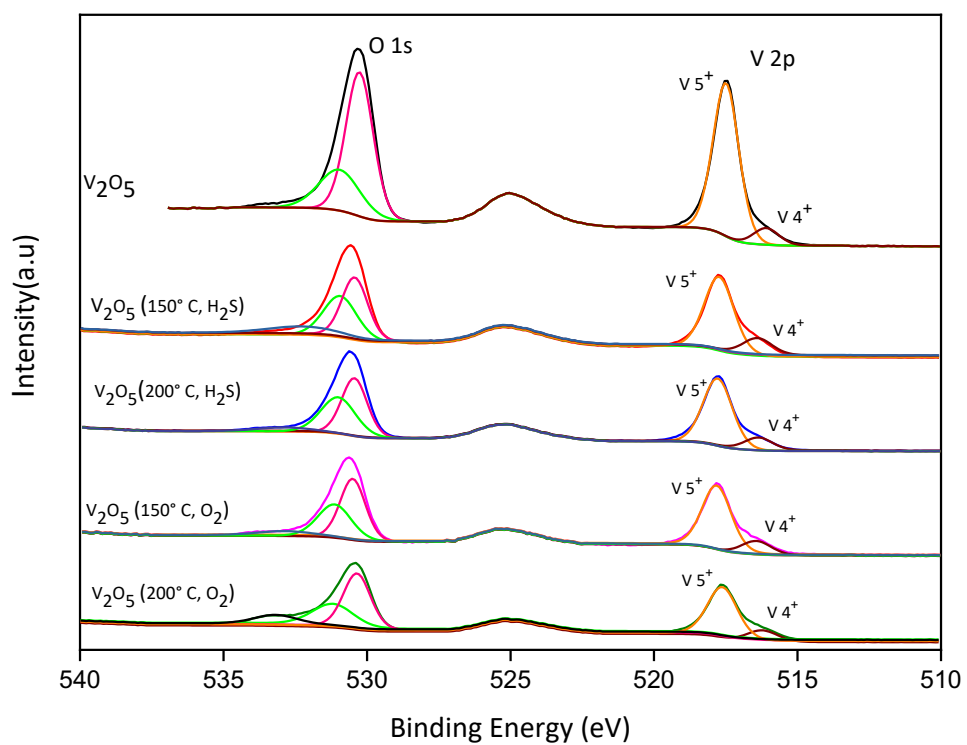


Figure 11. XPS study of V_2O_5 before and after reaction (V2p and O1s)

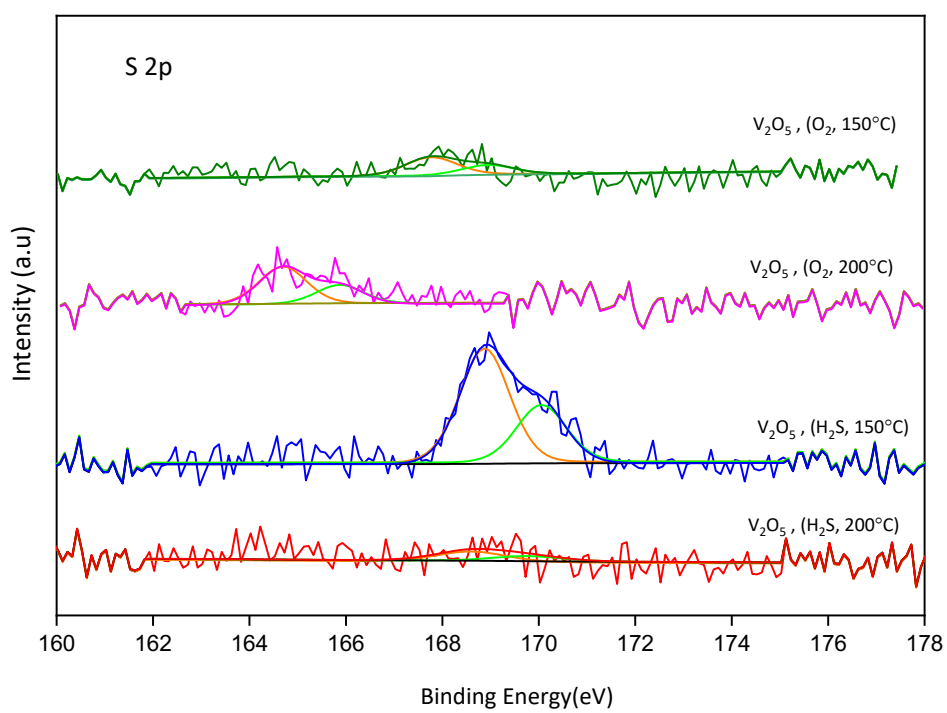


Figure 12. XPS study of V_2O_5 before and after reaction (S 2p)

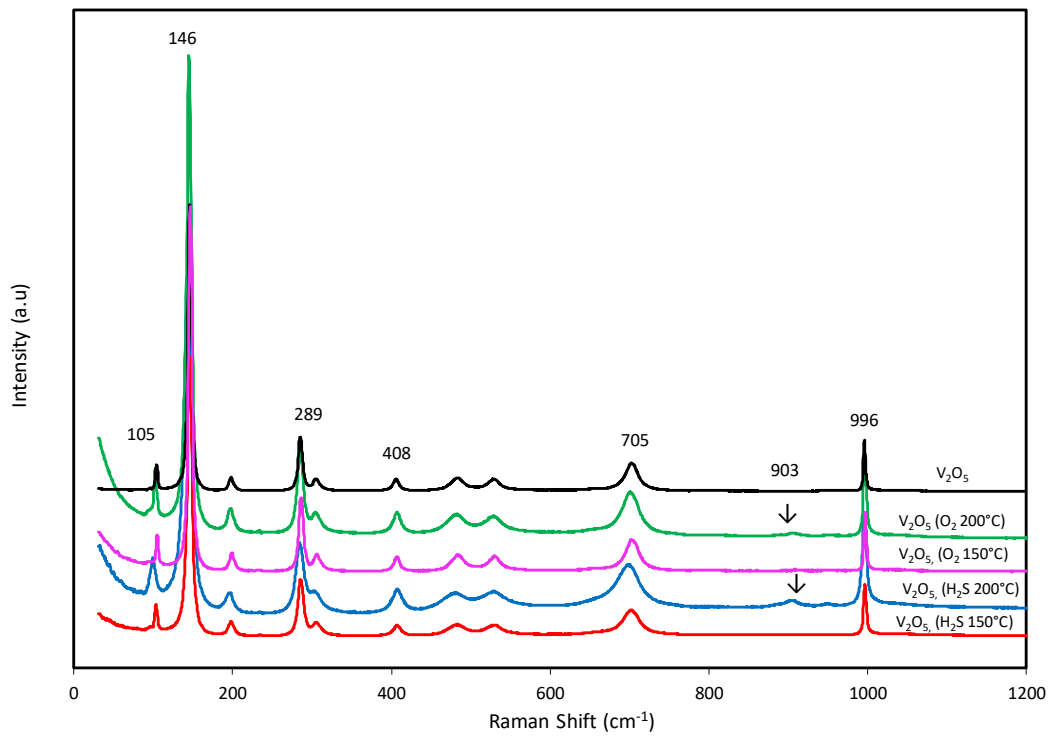


Figure 13. Raman study of V_2O_5 before and after the reaction

Operating Conditions	
Temperature	150-200 °C.
Carrier amount	80 mg V ₂ O ₅ + 900 mg SiC
H ₂ S Concentration	1000, 2000, 4000 ppm
H ₂ S:O ₂	1:5, 1:2.5, 1:0.5
CH ₄ (vol %)	20%
Cyclic operation	Step 1: 1 min in H ₂ S + He + Ar Step 2: 2 min in Ar Step 3: 1 min in O ₂ + He + Ar Step 4: 2 min in Ar
Total flow	100 mL min ⁻¹

Table 1. Operating condition for Chemical looping process

Temp (°C)	H ₂ S ppm	O ₂ ppm	H ₂ S:O ₂	T0 (min)			T30 (min)			T90 (min)		
				H ₂ S	O ₂	SO ₂	H ₂ S	O ₂	SO ₂	H ₂ S	O ₂	SO ₂
				Conv. (%)	Conv. (%)	Sel. (%)	Conv. (%)	Conv. (%)	Sel. (%)	Conv. (%)	Conv. (%)	Sel. (%)
150	2000	10000	1:5	98	10	1.8	89	68	13	75	7	13
200	2000	10000	1:5	98	25	31	98	18	27	97	17	24
150	2000	1000	1:0.5	97	96	1.4	77	64	4.7	45*	54*	6*
200	2000	1000	1:0.5	99	94	1.8	96	94	6.7	97	97	7.2

* Actual reaction time is 71 min,

Table 2. Co-feed catalytic oxidation of H₂S on bulk V₂O₅; 80 mg V₂O₅ + 900 mg SiC, F_T = 100 mL min⁻¹.

H₂S Concentration (ppm)	2000	2000	1000	4000	2000	2000
Temperature (°C)	150	200	150	150	150	150
H₂S:O₂	1:5	1:5	1:5	1:5	1:2.5	1:0.5
H₂S feed per cycle (μmol)	8.6	8.6	4.7	16.5	8.6	8.6
Conv H₂S (%)	82	85	86	63	76	71
H₂S converted (μmol)	7.1	7.3	4.0	10.4	6.5	6.1
S (μmol)	5.9	4.7	3.6	8.1	5.4	5.5
SO₂R (μmol)	0.4	1.1	0.1	0.5	0.3	0.3
SO₂O (μmol)	0.7	1.5	0.3	1.7	0.8	0.3
(S/S+SO₂R) (%)	94	81	96	94	95	95
%O_{latt} (% V⁵⁺ -> V⁴⁺)	1.6	1.8	0.9	2.2	1.4	1.4

Table 3. Summary of the results for CL oxidation of H₂S in various experimental conditions; 80 mg V₂O₅ + 900 mg SiC; T = 150 or 200 °C; H₂S concentration = 1000, 2000 or 4000 ppm; H₂S:O₂ ratio = 1:5, 1:2.5 or 1:0.5

Carrier	B.E (eV)		$V^{4+}/$ ($V^{4+}+V^{5+}$)	$V^{5+}/$ ($V^{4+}+V^{5+}$)	V^{4+}/V^{5+}	S/V
	V 2p					
	V^{4+}	V^{5+}				
V_2O_5	516.09	517.49	0.065	0.93	0.071	-
V_2O_5 150 °C H_2S	516.39	517.73	0.18	0.82	0.22	0.02
V_2O_5 200 °C H_2S	516.33	517.78	0.15	0.85	0.17	-
V_2O_5 150 °C O_2	515.97	517.39	0.17	0.83	0.19	
V_2O_5 200 °C O_2	516.17	517.62	0.19	0.81	0.23	-

Table 4. XPS analysis of samples before and after reaction, distribution of V^{4+} and V^{5+} species.

Supplementary Information

H₂S chemical looping selective and preferential oxidation to sulfur by bulk V₂O₅

Tanushree Kane, Jesús Guerrero-Caballero, Axel Löfberg

Univ. Lille, CNRS, Centrale Lille, ENSCL, Univ. Artois, UMR 8181 - UCCS - Unité de Catalyse et Chimie du Solide, F-59000 Lille, France

2. Experimental sections

2.3 Reactivity tests for H₂S selective oxidation.

Additional detailed experimental setup description

The reactor setup is represented in Figure S1.

The reactor is U shaped quartz tube (6 mm O.D.) and a larger space (12mm O.D., 10mm I.D.) containing a fritted disc defining a volume of approx. 2 mL in which the catalyst/oxygen carrier is placed. The reactor is placed in a temperature regulated furnace. A thermocouple is placed against the outer wall of the reactor at the catalyst/carrier level for temperature recording.

A Pyrex glass tube (4 mm I.D.) is connected directly to the quartz reactor outlet in order to condense the sulfur produced during reaction ("Glass condenser"). This condenser was regularly replaced and cleaned to avoid plugging by condensed sulfur.

The reactor section composed of the reactor itself and glass condenser can be closed using 4-way valve V1. A second condenser is placed downstream of the reactor in order to ensure that no trace of sulfur remain that could be condensed in the analytical instrument. All lines (1/8" tubing) from V1 to the analytical instruments are heated at 200 °C (heating cords).

Gas streams are set using 6 mass flow controllers (MFC, Brooks 5980). MFC's n. 1, 4 and 6 are fed with Argon; MFC2 with H₂S/He mixture (premixed cylinder); MFC5 with O₂/He mixture (premixed cylinder) and MFC3 with pure methane (99.995%).

In *chemical looping mode*, 4-way valve V3 is fed by Ar (MFC1) and H₂S/He (MFC2) streams with equivalent flow rates. Similarly, V4 is fed by Ar (MFC6) and O₂/He (MFC5) streams with equivalent flow rates. Streams coming from V3 and V4 are then mixed with another Ar stream (MFC4). This allows to adjust "reductant" and "oxidant" concentrations independently in a wide range.

All 4-way valves (V1 to V4) are equipped with air actuators. During looping operation, valves V3 and V4 are operated sequentially using a homemade control system and software.

At all time the flow rate at reactor inlet is constant as it is composed of three components

$$\text{Total flow} = \text{MFC4} + (\text{MFC1 or MFC2}) + (\text{MFC5 or MFC6})$$

In co-feed mode, both V3 and V4 are switched to feed reactant gases together.

In preferential oxidation tests in presence of methane, a methane stream is added to the reductant line feeding V3 and Argon flows (MFC1 and MFC4) are adapted consequently.

In both reductant and oxidant steps, the He contained in the premixed cylinders acts as a tracer of the reactant stream.

Before and after each chemical looping sequence, a cycle is performed with reactor closed (V1 in by-pass position). This allows to calibrate the H₂S, O₂ and He responses. During reacting cycles (V1 in open reactor position) H₂S conversion can be determined by calculating the theoretical H₂S inlet curve using the He one.

Figure S2-A illustrates a typical example partial pressure evolution with time during Chemical Looping operation in these experimental conditions. Figure S2-B shows a detail of last cycle in presence of carrier and by-pass (reference) cycle.

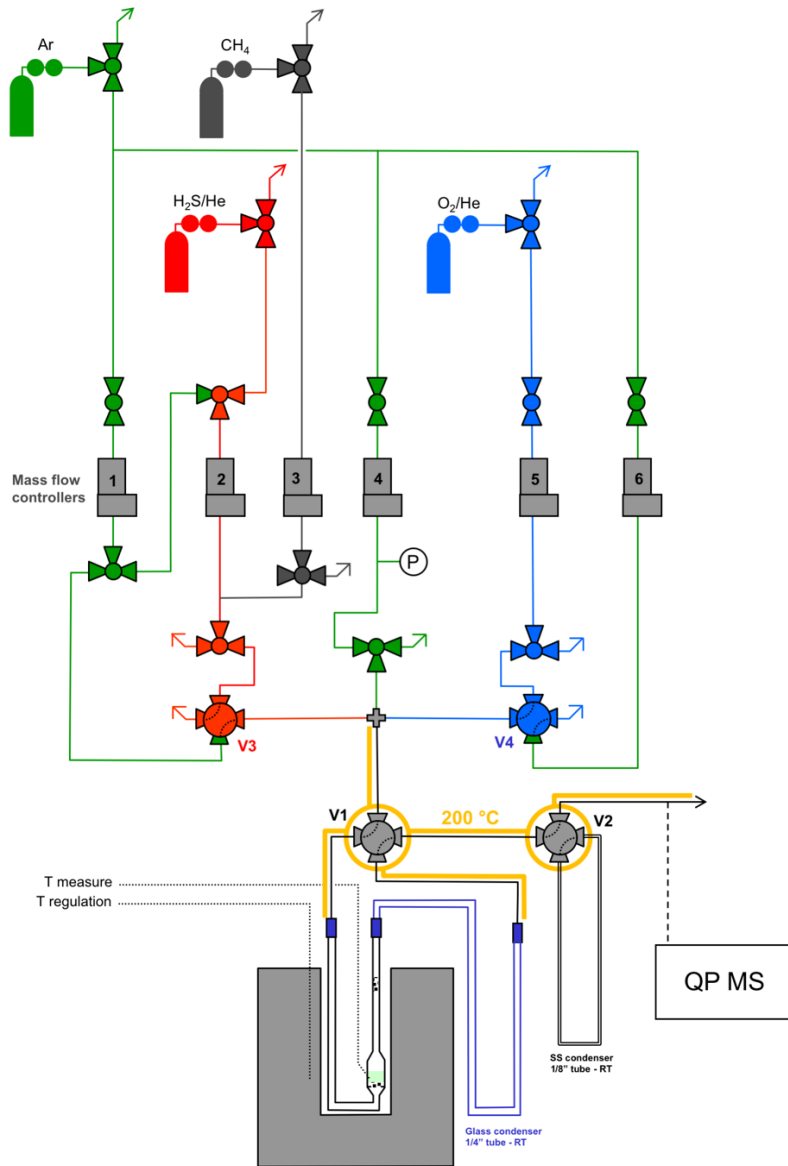


Figure S1. Reactor setup scheme

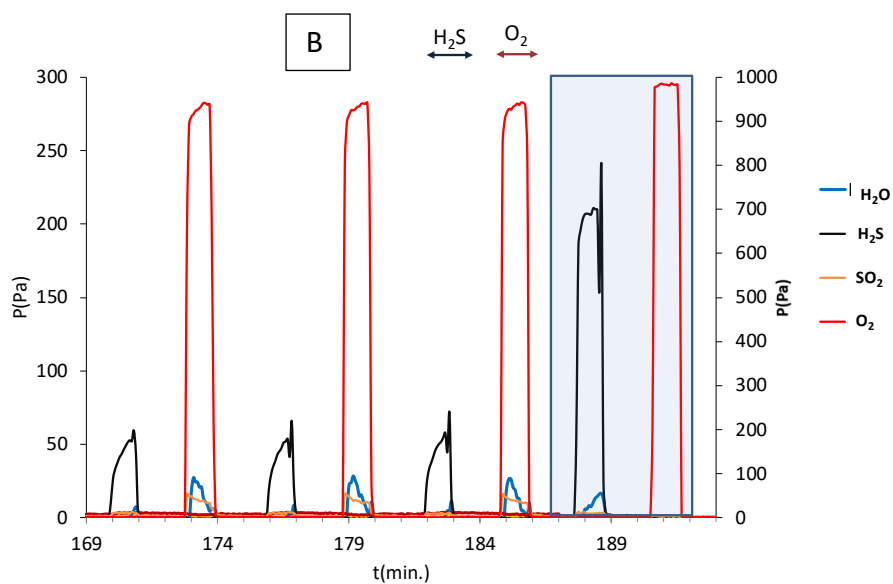
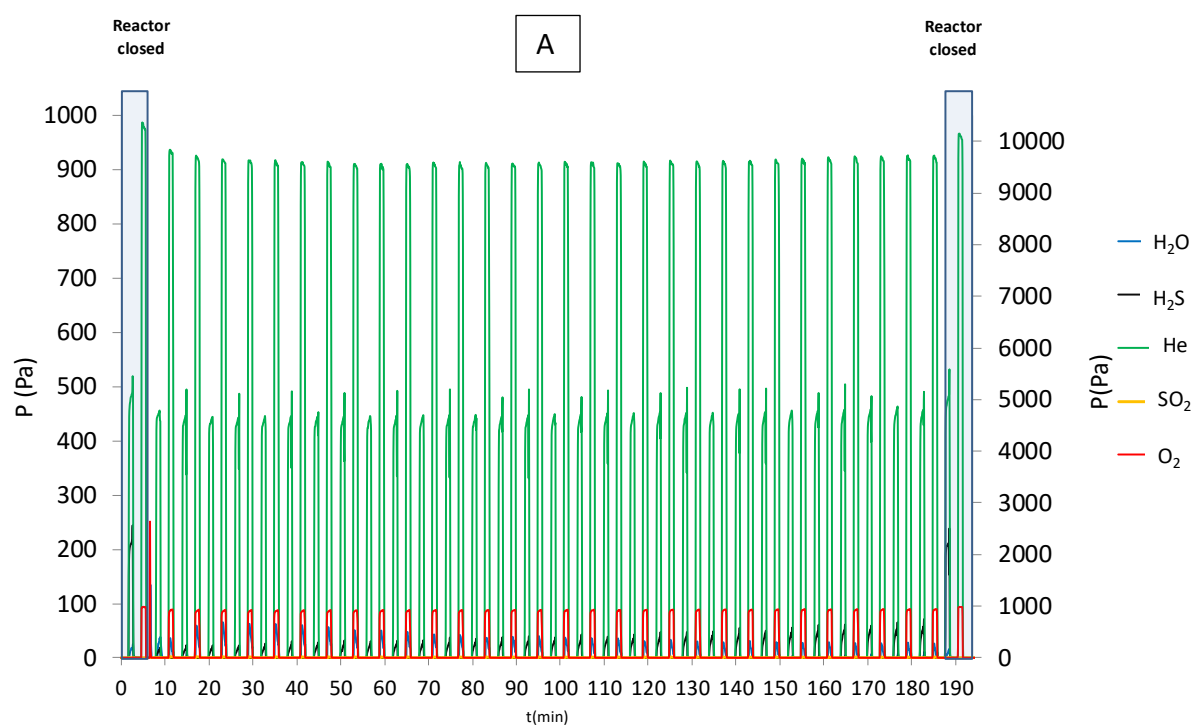


Figure S2. Partial pressures evolution during H₂S – O₂ cycling
 80 mg V₂O₅ + 900 mg SiC at 150 °C, F_T = 100 mL min⁻¹
 Cycle: 1min. in 2000 ppm (200 Pa) of H₂S and 1 min. in 10000 ppm (1000 Pa) of O₂
 H₂S:O₂ = 1:5
 A: overall view on full experiment (30 cycles)
 B: detail of partial pressure evolution for the last 3 cycles.

3.2. Performances in co-feed catalytic H₂S selective oxidation.

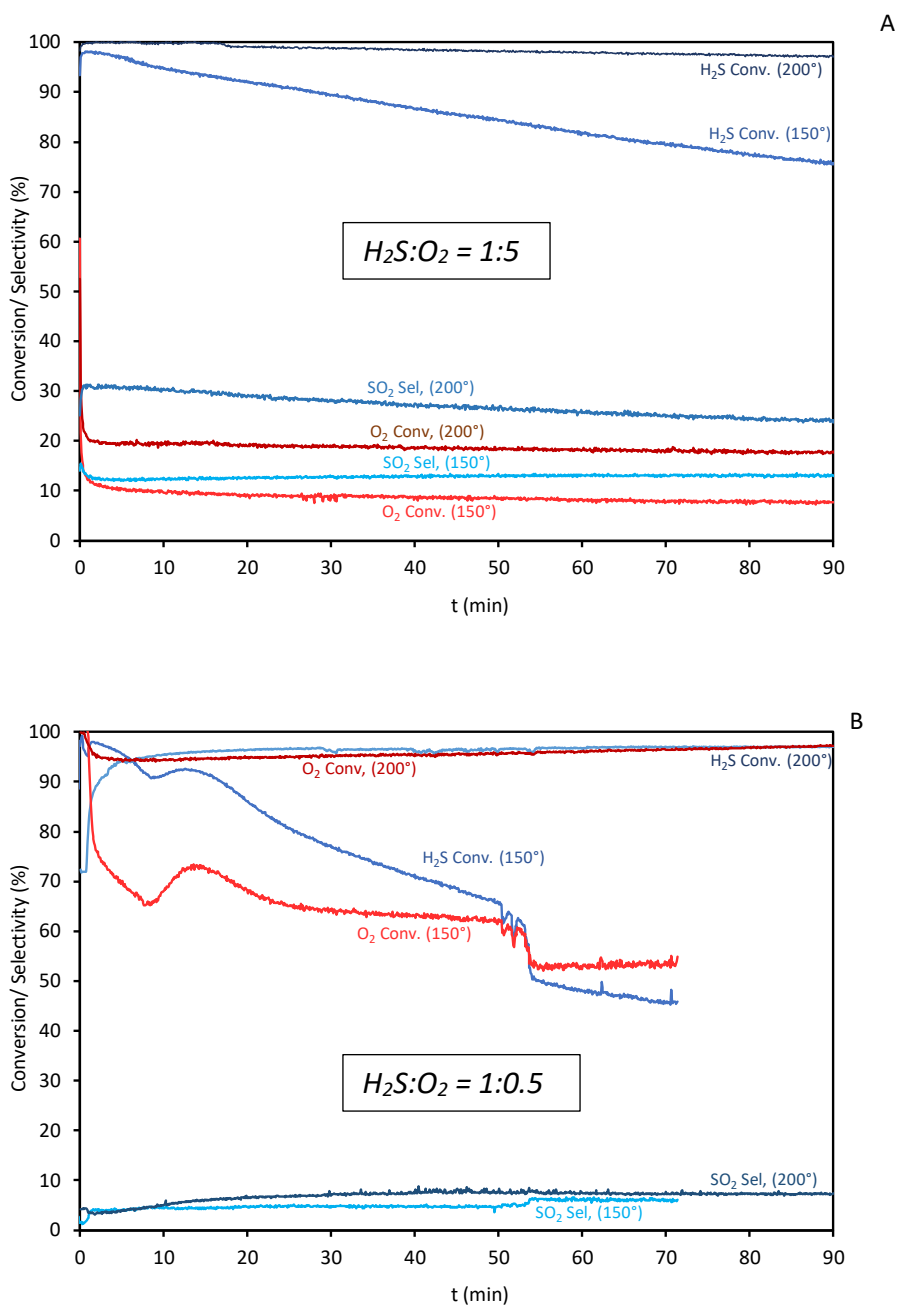


Figure S3. Evolution of H₂S and O₂ conversion and SO₂ selectivity in co-feed H₂S oxidation
 80 mg V₂O₅ + 900 mg SiC at 150 °C and 200 °C, $F_T = 100 \text{ mL min}^{-1}$,
 A: $H_2S:O_2 = 1:5$ (2000 ppm of H₂S, and 10000 ppm of O₂,)
 B: $H_2S:O_2 = 1:0.5$ (2000 ppm of H₂S, and 1000 ppm of O₂)

3.3.4 Reactivity in presence of methane

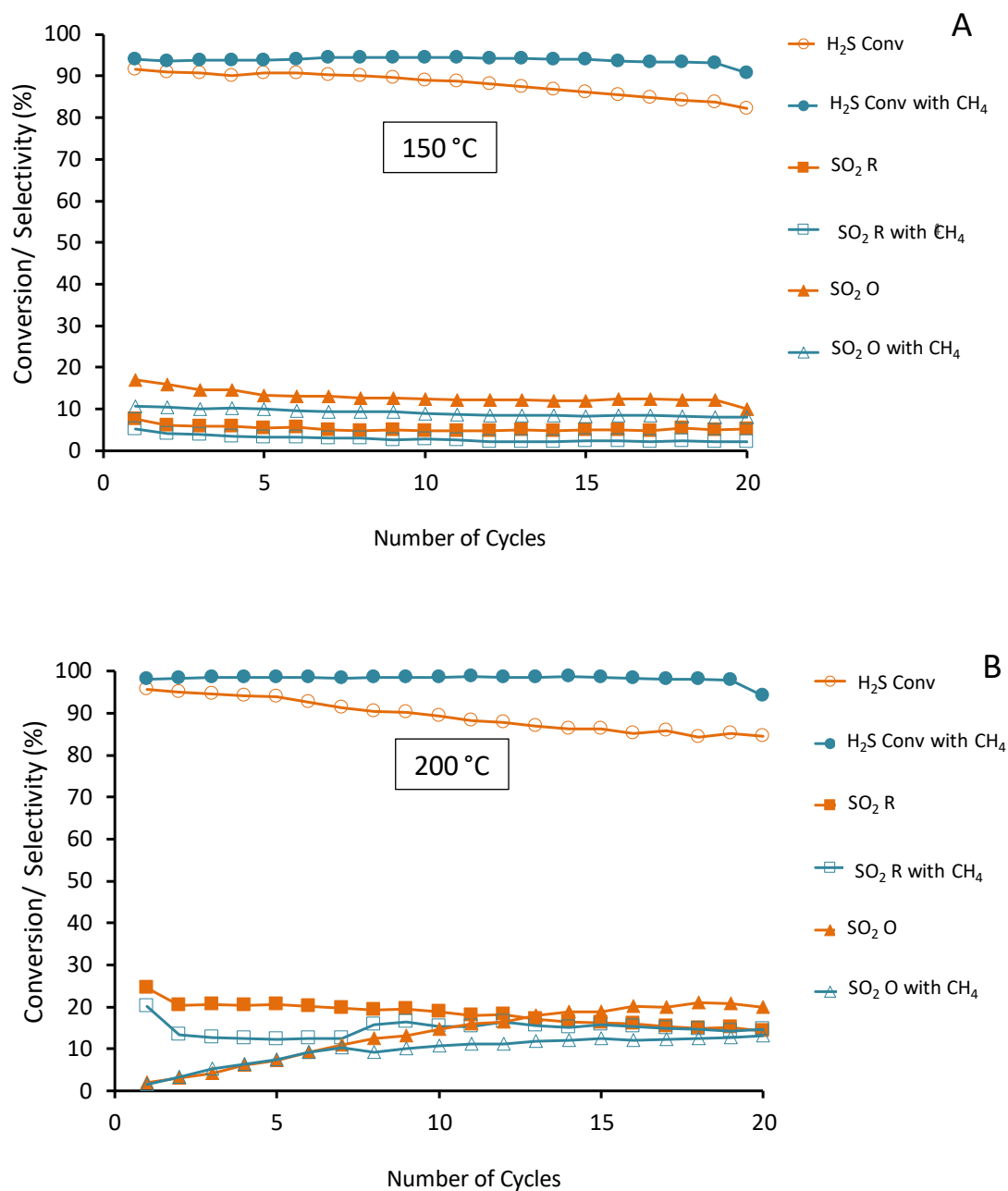


Figure S4. Chemical looping preferential oxidation of H₂S in presence of CH₄

80 mg V₂O₅ + 900 mg SiC, F_T = 100 mL min⁻¹, 2000 ppm of H₂S, H₂S:O₂ = 1:5, CH₄ = 20 %

Closed symbol (•) without CH₄, open symbol (o) with CH₄

A: T=150 °C

B: T=200 °C